



# Treball Final de Grau

**Intramolecular dehydration of 5-nonanol over ion exchange resins.**

Victòria Cabot de Pomés

*June 2020*



UNIVERSITAT DE  
BARCELONA



Aquesta obra està subjecta a la llicència de:  
Reconeixement-NoComercial-SenseObraDerivada



<http://creativecommons.org/licenses/by-nc-nd/3.0/es/>



*Continuous effort -not strength or intelligence- is  
the key to unlocking our potential.*

Winston Churchill

Agraeixo a la meva família pel seu suport incondicional al llarg d'aquesta etapa. Sempre he pogut comptar amb la seva ajuda i els seus savis consells. En especial a la meva germana per tot i estar a quilòmetres de distància trobar temps per donar-me el seu suport.

Als amics i a la meva parella per la seva paciència i compressió durant aquest viatge.

Al departament de Cinètica i Catàlisis Aplicada per obrir-me les portes i facilitar-me la tasca en tot moment.

Al Dr Roger Bringué i la Dra Eliana Ramírez pel seu interès demostrat i la seva ajuda, he pogut comptar amb ells en tot moment quasi es podria dir que a totes hores. La seva expertesa i coneixements han estat fonamentals i de gran guia per la realització del treball a més han aconseguit fer més agradable aquest llarg període de confinament.

Gràcies.



# CONTENTS

SUMMARY .....	I
RESUM.....	II
1. INTRODUCTION .....	1
1.1. BIOFUELS.....	2
1.1.1. TYPES OF BIOFUELS.....	2
1.1.2. SECOND GENERATION BIOFUELS (SGB) .....	3
1.2. FROM LEVULINIC ACID TO NONENES .....	5
1.2.1. THE USE OF NONENES .....	7
1.2.2. NONENES AS DIESEL FUEL.....	8
1.2.3. NONENES FOR GASOLINE BLENDING.....	10
1.3. CATALYSIS .....	11
1.4. STATE OF THE ART OF NONENES PRODUCTION BY ALCOHOL DEHYDRATION .....	14
2. OBJECTIVES.....	16
3. EXPERIMENTAL SECTION.....	17
3.1 EXPERIMENTAL SETUP .....	20
3.1.1. ANALYTICAL SYSTEM .....	21
3.2 EXPERIMENTAL PROCEDURE .....	23
3.2.1. RESIN PRETREATMENT .....	23
3.2.2. REACTOR LOADING .....	23
3.2.3. EXPERIMENT LAUNCHING .....	24
3.2.4. SAMPLING .....	24
3.2.5. CLEAN-UP .....	25
3.3. EXPERIMENTAL CONDITIONS.....	25
3.3.1 OTHER EXPERIMENTS .....	26
4. GENERAL CALCULATIONS.....	28
5. RESULTS AND DISCUSSION.....	30
5.1. REACTION ASSESSMENT .....	30

5.1.1	EVALUATION OF THE EXPERIMENTAL ERROR .....	33
5.2.	EXPERIMENTAL STUDY WITH DIFFERENT RESINS .....	34
5.3.	EXPERIMENTAL STUDY WITH A45 AT DIFFERENT TEMPERATURES .....	41
5.4.	DETERMINATION OF APPARENT ACTIVATION ENERGY .....	44
6.	CONCLUSIONS .....	46
	REFERENCES AND NOTES: .....	47
	ACRONYMS .....	50



## SUMMARY

Due to increasing environmental awareness as well as diminishing oil reserves, in recent years, pathways to obtaining renewable chemicals have been studied. One of the clearest pathways is to obtain bio-chemicals from lignocellulose. It consists mainly of lignin, hexoses and pentoses. A very wide range of reactions to obtain bio-chemicals is opened from hexoses (glucose, etc.) and pentoses (fructose, etc.). One of these pathways is the formation of alkenes from levulinic acid. It is a serial reaction system that undergoes the formation of  $\gamma$ -valero lactone, pentanoic acid and 5-nonanone. Later 5-nonanone is hydrogenated to obtain 5-nonanol, which is the starting point of the reaction that we propose to study: the dehydration of 5-nonanol to nonenes using ion exchange resins as catalysts. Nonenes are usually used to improve the gasoline blending.

The reaction, discussed above, will be studied by performing catalyst screening and working with different reaction temperatures in a stirred tank batch reactor with the purpose of maximizing nonene production.

The research clearly indicates that the catalytic reaction takes place mostly on the outer surface of the ion-exchange resins. Studied resins with different structural property yielded similar results in terms of selectivity. A mixture of nonenes were obtained, but no side-reactions were detected. The acid capacity of the resins is the most relevant property: the greater the acid capacity the higher the conversion of 5-nonanol. Thus, at 150°C, the highest alcohol conversion and reaction rate was obtained over Amberlyst 35. Furthermore, the reaction was studied in the temperature range 140-180°C over the thermostable resin Amberlyst 45. As expected, both alcohol conversion and reaction rate increased with temperature, with a selectivity of 100% to nonenes. The activation energy was estimated to be 138 kJ/mol.

**Keywords:** Nonenes; ion-exchange resins; bio-chemicals, 5-nonanol dehydration



## RESUM

Degut a l'augment de la consciència ambiental, així com a la disminució de les reserves del petroli, s'estan estudiant, en els últims anys, vies per l'obtenció de productes químics d'origen renovable. Una de les vies més clares és l'obtenció de bioproductes a partir de la lignocel·lulosa. Aquesta està formada principalment per lignina, hexoses i pentoses. A partir de les hexoses (glucosa, etc.) i pentoses (fructosa, etc.) sobre un ventall molt gran de reaccions per a obtenir bioproductes. Una d'aquestes vies és la formació d'alquens a partir de l'àcid levulínic. Es tracta d'un sistema de reaccions en sèrie que passa per la formació de la  $\gamma$ -valero lactona, l'àcid pentanoic i la 5-nonanona. Aquesta última s'hidrogena per a obtenir el 5-nonanol, que és el punt de partida de la reacció que es proposa estudiar: la deshidratació del 5-nonanol a nonenes utilitzant resines de bescanvi iònic com a catalitzadors.

La reacció, comentada anteriorment, s'analitzarà realitzant un estudi dels catalitzadors i de les condicions d'operacions més adients per tal de maximitzar la producció de nonens en un reactor discontinu tanc agitat amb el propòsit de maximitzar la producció de nonens.

La recerca clarament indica que la reacció catalítica té lloc majoritàriament en la superfície exterior de les resines d'intercanvi iònic. Les resines estudiades amb diferents propietats estructurals varen cedir resultats similars en termes de selectivitat. Es va obtenir una mescla de nonenes, però cap reacció secundària. La capacitat àcida de les resines és la propietat més rellevant: com més gran és la capacitat àcida més gran és la conversió de 5-nonanol. Així, a 150 °C, és va obtenir la major conversió d'alcohol i la major velocitat de reacció sobre Amberlyst 35. Com era d'esperar, tant la conversió d'alcohol com la velocitat de reacció van incrementar amb la temperatura amb una selectivitat de 100% cap a nonenes. L'energia d'activació establerta va ser 138 kJ/kmol.

**Paraules clau:** Nonenes, resines d'intercanvi iònic, bioproductes, deshidratació de 5-nonanol



# 1. INTRODUCTION

Climate change is here, and the wide range of impacts makes it one of the biggest risks facing humanity today. Burning fossil fuels generates a large amount of carbon dioxide in the atmosphere which is a greenhouse gas (GHG). Even though the emission of GHG is not the only factor affecting climate change is currently the biggest contributor given that it produces the greenhouse effect which makes the earth warmer. In 2017, almost 30% of the greenhouse gas emissions came from Transportation becoming the second largest responsible Industry with majority of GHG emissions. Within this sector, road transportation is the biggest contributor with more than a 70% of greenhouse gas emission as shown in Figure 1 (Directive, 2019; Todts, 2018). The European directive 2009/30 / EC was established as a measure with new regulations on fuels quality, which from now on cannot emit more than a quantity of GHG. To comply with this directive, the use of renewable energy sources was proposed (European Environment Agency, 2019; Parliament & Union, 2009).

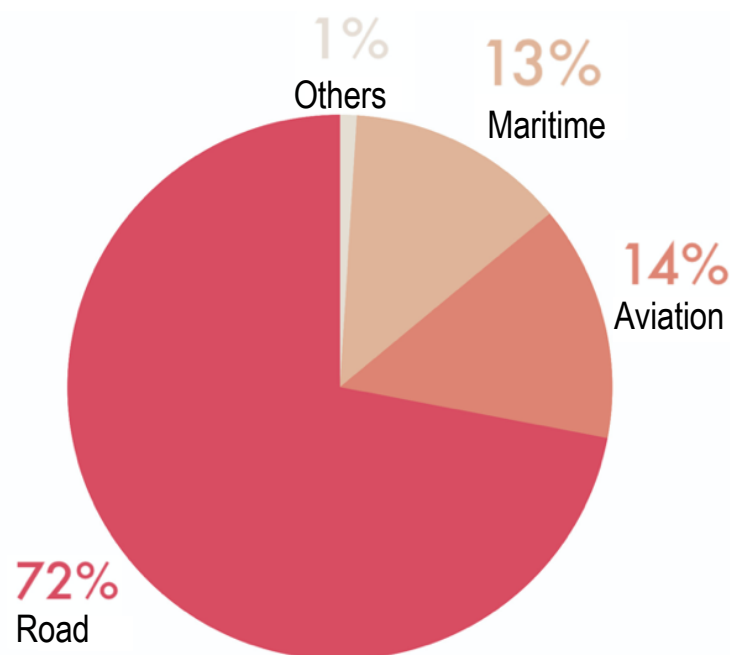


Fig 1. EU(Convention)-Share of transport greenhouse gas emissions 2017.

(Image adapted from European Environment Agency (2019))

Currently, the major source of energy comes from fossil fuels. Among these, oil is the most consumed, followed by coal and then natural gas. These energy sources cannot be considered renewable energy because the current used sources will be depleted and will not be replenished for thousands or even millions of years. Furthermore, while fossil fuels are a valuable and efficient source of energy, they are harmful to the environment since the combustion process occurs so fast that living plants and trees are not sufficient to reabsorb all the carbon dioxide emitted to the atmosphere. A promising alternative to petroleum is the use of biomass for the production of biofuel (Binod et al., 2019). Biofuels are considered a renewable energy because it generates bioenergy by a net carbon balance making it benign to the environment.

## 1.1. BIOFUELS

Biofuel is a fuel which uses biomass as feedstock to be produced. They are one of the alternatives to the use of fossil fuels. However, we could not completely replace fossil fuels with biofuels because they are not enough to supply the entire population.

The process of obtaining biofuel is by net balance of carbonate dioxide, which means that the carbon released by the burning of biofuels is the same carbon that will be reabsorbed and used for cellular respiration through the cultivation of vegetation, which will be then used to produce more biofuel thus closing the carbon life cycle (Axelsson et al., 2008).

### 1.1.1. TYPES OF BIOFUELS

There are four different types of biofuel depending on the biomass origin:

**First Generation Biofuels (FGB)** use edible crops as biomass to be produced. This type of biofuel is well-known because it uses available technology to be generated. Nevertheless, FGB is illegal in some countries because they have a negative impact decreasing the availability of food and contributing to food price increase.

**Second Generation Biofuels (SGB)** use nonedible crops to produce the biomass, by preference from lignocellulose. This type of biofuels have a high cost due to its complexity of sugar extraction (Tejero et al., 2016).

**Third Generation Biofuels (TGB)** are derived from algae, the problem is that in order to generate them a high quantity of phosphates is needed which makes it an unaffordable

process. These generations are always limited due to the corresponding availability of organic raw material, biomass, thus limiting its application on a global scale.

**The Fourth Generation Biofuels** are directly derived from solar energy by synthetic biology. Unlike the other generations, the feedstock being used is inexhaustible, inexpensive and does not have availability problems. On the other hand, they present difficulties on the obtention and extra costs derived from the control and management of these given that we will be working with biologic systems. The fourth generation is a possible route but currently more expensive and less competitive.

SGB biofuel will be the focal point of this project.

### **1.1.2. Second Generation Biofuels (SGB)**

The second generation biofuels have the main advantage of not competing with the food industry. Furthermore the biomass used in this generation of recycled materials from forest, agricultural, agro-industrial and food, these could cause environmental problems if they are not properly recycled (Maitan-Alfnas et al., 2015). On the other hand, they have some limitations, the most relevant is the increase in production cost due to the need for complex technologies since the plants used as a biomass in the production of SGB have lignocellulose as a structural element. Lignocellulose is composed of cellulose, hemicellulose, lignin and inorganic salts, due to their hydrogen bonds, provides structural resistance to the plants, hindering its biological and chemical degradation (Pileidis & Titirici, 2016).

There is a large number of substances that can be obtained through biomass, among them 12 basic substance stand out as shown in Table 1, which will later become high-quality chemical or biological components (Werpy & Petersen, 2004).

Table 1. 12 Basic building blocks from biomass and uses.

*(Table adapted from Werpy & Petersen (2004))*

BUILDING BLOCKS	DIRECT USE	POTENTIAL USE OF DERIVATIVES
1,4 succinic, fumaric and malic acids	---	Solvents, green solvents, water soluble polymers (water treatment), fibers
2,5 furan dicarboxylic acid	Polyester	Polymers
3 hydroxy propionic acid	---	Super Absorbent Polymers (SAP) for diapers, contact lenses, fibers
Aspartic acid	Sweeteners	Amino analogs of C4 1,4 dicarboxylic acids
Glucaric acid		Solvents, Nylons
Glutamic acid	---	Monomers for polyesters and polyamides
Itaconic acid	Copolymers	Confer new useful properties of polymers, solvents and polymer precursor
Levulinic acid	---	Biofuels, solvents, copolymerization, replacement for bisphenol
3-hydroxybutyrolactone	Intermediate pharma compounds	Solvents, Amino analogs to lycra fibers
Glycerol	Pharmaceuticals, foods/beverages, and polyether polyols	Thermopolymer, Polyester fibers, Antifreeze, humectant,
Sorbitol	---	Polymer, antifreeze
Xylitol/arabinitol	Non-nutritive sweeteners, anhydrosugars, unsaturated polyester resins (UPRs)	Polymer, antifreeze

In particular, levulinic acid (LA) is the most important bio-derived molecule that can be transformed into various biofuels and valuable chemicals (Wettstein et al., 2012). The obtention of LA through biomass can be seen in Figure 2.



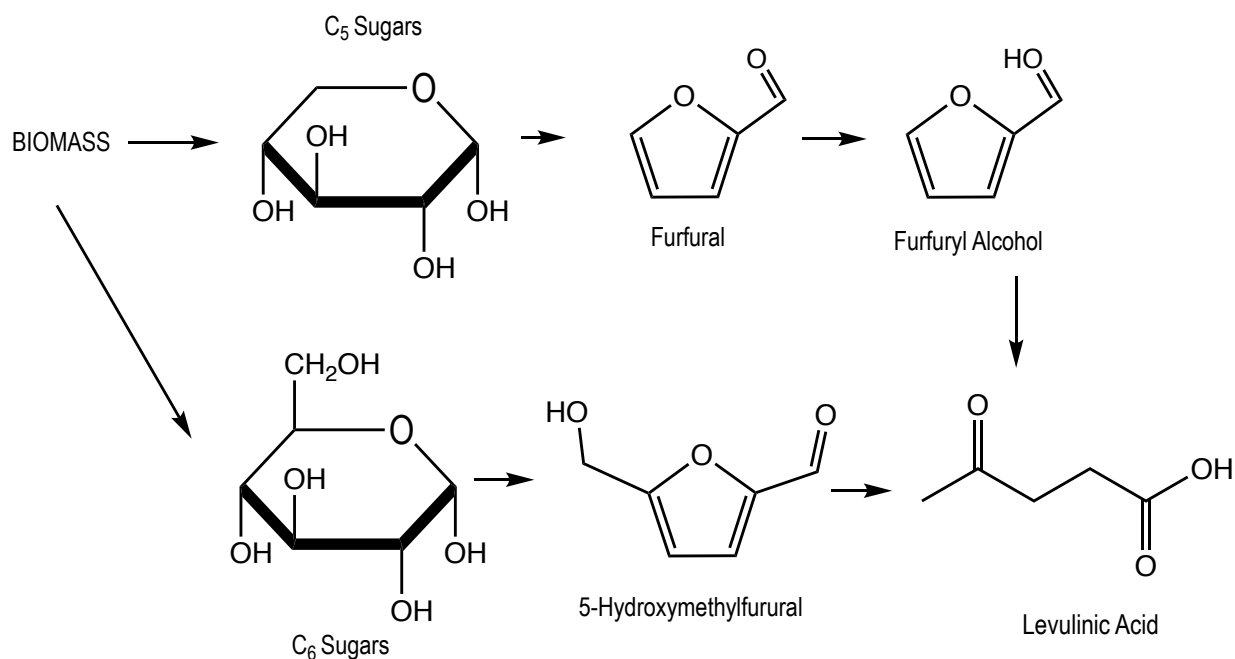


Fig 2. From biomass to LA

(image adapted from Yan et al. (2017))

## 1.2. FROM LEVULINIC ACID TO NONENES

Levulinic acid is obtained by acid hydrolysis of lignocellulosic biomass. The process of hydrolysis can be done in two different ways, by the use of acids or the most innovative which is by the use of enzymes. The use of enzymatic hydrolysis requires less energy which makes the use of this process a more ecofriendly option (Maitan-Alfenas et al., 2015).

One important derivative from levulinic acid is the  $\gamma$ -valero lactone (GVL) due to its properties which makes it a stable and reactive component for the production of valuable chemicals, among them the 5-nonanone. The process for obtaining GVL from LA can be through two different pathways (see Figure 3), on one hand we have the hydrogenation of LA that leads to the formation of  $\gamma$ -hydroxy valeric acid which is followed by an esterification and the loss of a water molecule to form GVL. At the same time, the second route begins with the dehydration of LA to obtain angelica lactone that via a hydrogenation produces GVL (Wettstein et al., 2012).

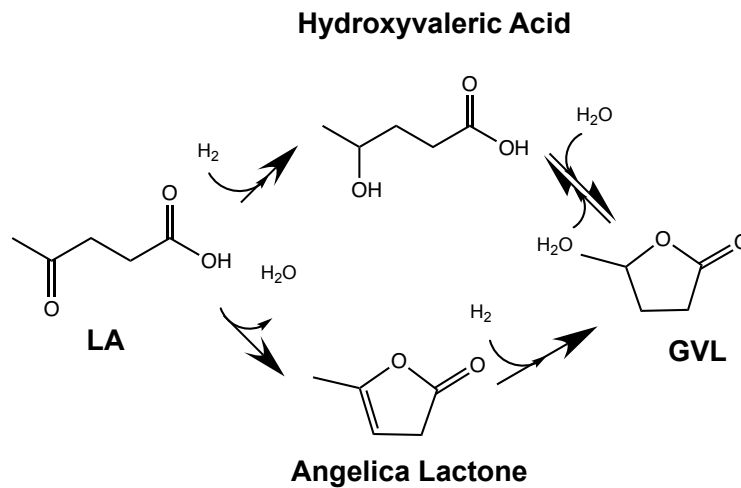


Fig 3. The two pathways for GVL production.

(image adapted from Serrano-Ruiz et al.(2010))

The hydrogenation of GVL produces pentanoic acid via the ketonization reaction to 5-nonanone. Finally, the process for obtaining linear C<sub>9</sub> alkenes (nonenes) is by the sequential hydrogenation and dehydration reaction of C<sub>9</sub> ketone (see Figure 4) (Wettstein et al., 2012).

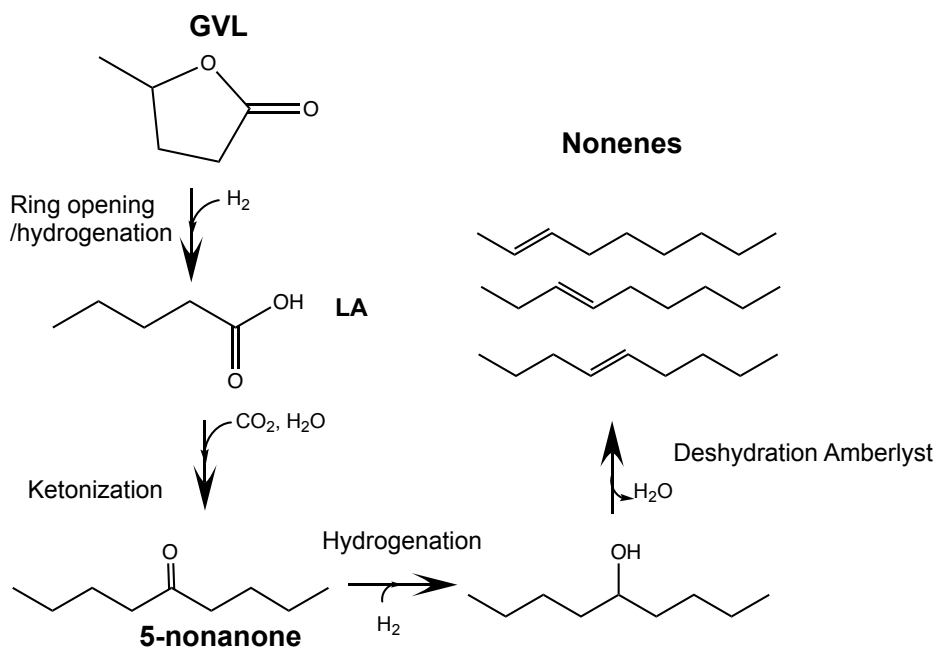


Fig 4. Reaction for conversion of GVL to Nonenes.

(image adapted from Alonso et al. (2010))

### 1.2.1. The use of nonenes

Nonenes are olefins (alkenes) which are defined as hydrocarbons with one or several carbon-to-carbon double bonds (C=C), with C<sub>9</sub>H<sub>18</sub> as their molecular formula.

A nonene is considered as a higher molecular weight olefin which is defined as an alkene with more than seven carbons. These types of olefins are used as a basic component for the production of intermediate and end products like some special alcohols or detergents (02/03/2020, ExxonMobil Chemical, n.d.).

Nonenes can also be known as plasticizers, additives that decrease the plasticity or viscosity of a material. Accordingly, nonenes can also be used in the polymer industry as an additive, for instance to improve flexibility of rigid plastics as in the production of polyvinyl chloride (PVC) (05/03/2020, Shell Chemicals, n.d.).

Alkenes such as hexenes, heptenes, octenes, nonenes and decenes can be used as aromatics (Khaled, A; Robert, 2002).

Nonenes may be hydrogenated to obtain n-nonanes (alkane) which are linear hydrocarbons that can be used as components for gasoline and diesel as discussed by Alonso et al (2010). Furthermore, via oligomerization and afterwards hydrogenation reactions of nonenes it produces C<sub>18</sub> alkanes which can be used as jet fuel and also for diesel (see Figure 5) (Alonso et al., 2010; Blanca Torrubia Chalmeta, 2010; Chen et al., 2013)

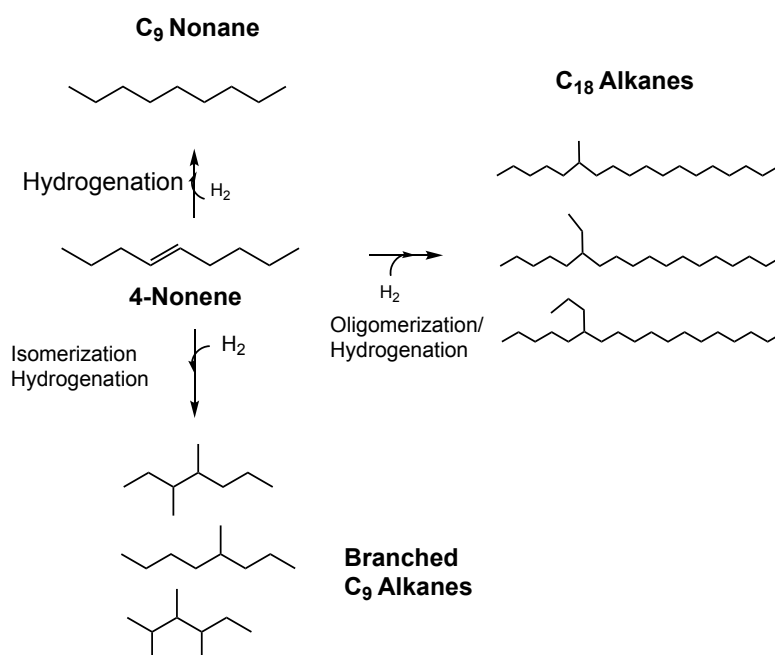


Fig 5. 4-Nonene to C<sub>9</sub> and C<sub>18</sub> alkenes.

(image adapted from Ramírez et al. (2017))

## 1.2.2. Nonenes as diesel fuel

Nonane and its oligomerization are hydrocarbons that contain only carbon-carbon single bonds and are known as normal paraffins or alkanes. In gasoline, the carbon range goes from 4 to 12, while diesel contains approximately 12 to 25 carbon atoms. For these reason nonane can be used for diesel and for gasoline and their oligomerization ( $>C_9$ ) is used as diesel.

Diesel is a blend of a large number of components mostly paraffins (alkanes), aromatics and naphthenes (hydrocarbons that are known as cycloalkanes if they are cyclic). Each component type adds a different physical property to the fuels.

There are various types of diesel, each one determined by their differences in composition based on the compounds percentages added to the blend (Gürbilek, 2013).

Depending on the purpose, nonane as n-paraffin can be used in the blend of the diesel to improve its properties. By modifying the following physical properties within each blend, we can obtain different types of diesel fuel:

**Boiling Point:** Increases with the carbon number.

**Freezing Point:** Increases with molecular weight and depends on the molecular shaper. This makes n-paraffins the component with the higher melting point compared with others.

**Density:** Increases with carbon number. In case that the number of carbons is the same we can increase it by using paraffins.

**Heating Value:** Increases with carbon number (Miranda et al., 2015). On a weight basis, the order heating value increases by class with aromatic being the highest and paraffin the lowest.

**Cetane Number:** In general, paraffins have high cetane number which increases with molecular weight.

**Viscosity:** Depends only on the molecular weight. Having higher viscosity in naphthenes than in paraffins or aromatics.

Finally, if we compare the main components of diesel (see Table 2), we conclude that n-paraffins have an outstanding cetane number (Gürbilek, 2013).

Table 2. Cetane number of the different pure components.

*(Table adapted from Rosinski & Olsen (2009))*

	<b>Compound</b>	<b>Formula</b>	<b>Cetane number</b>
<b>n-Paraffins</b>	n-Decane	C <sub>10</sub> H <sub>22</sub>	76
	n-Pentadecane	C <sub>15</sub> H <sub>32</sub>	95
	n-Hexadecane	C <sub>16</sub> H <sub>34</sub>	100
	n-Eicosane	C <sub>20</sub> H <sub>42</sub>	110
<b>Isoparaffins</b>	3-Ethyldecane	C <sub>12</sub> H <sub>26</sub>	48
	4,5-Diethyloctane	C <sub>12</sub> H <sub>26</sub>	20
	Heptamethylnonane	C <sub>16</sub> H <sub>34</sub>	15
	8-Propylpentadecane	C <sub>18</sub> H <sub>38</sub>	48
	7,8-Diethyltetradecane	C <sub>18</sub> H <sub>38</sub>	67
	9,10-Dimethyloctadecane	C <sub>20</sub> H <sub>42</sub>	59
<b>Naphthenes</b>	Decalin	C <sub>10</sub> H <sub>18</sub>	48
	3-Cyclohexylhexane	C <sub>12</sub> H <sub>24</sub>	36
	2-Methyl-3-cyclohexylnonane	C <sub>16</sub> H <sub>32</sub>	70
	2-Cyclohexyltetradecane	C <sub>20</sub> H <sub>40</sub>	57
<b>Aromatics</b>	1-Methylnaphthalene	C <sub>11</sub> H <sub>10</sub>	0
	n-Pentylbenzene	C <sub>11</sub> H <sub>16</sub>	8
	Biphenyl	C <sub>12</sub> H <sub>10</sub>	21
	1-Butynaphthalene	C <sub>14</sub> H <sub>16</sub>	6
	n-Nonylbenzene	C <sub>15</sub> H <sub>24</sub>	50
	2-Octylnaphthalene	C <sub>18</sub> H <sub>24</sub>	18
	n-Tetradecylbenzene	C <sub>20</sub> H <sub>34</sub>	72

In addition, the greenhouse gases emitted in the diesel fuel process, including SO<sub>x</sub>, NO<sub>x</sub> and CO<sub>2</sub>, must be reduced if we want to comply with the standards of Directive 2009/30 / EC of the European Parliament and of the Council of April 23, 2009. The solution to this problem is through the use of fuel formed from diesel-biodiesel blends and jet fuel, which would represent a fuel with stable operation and a lower percentage of greenhouse gas emissions (Ashour & Elwardany, 2020; Balamurugan & Nalini, 2016). This is because biodiesel is considered a renewable energy, therefore, as mentioned above, it does not emit more CO<sub>2</sub> into the atmosphere. Furthermore, the production of biodiesel is made by adding bio-paraffins, such as nonane and those obtained by

oligomerization of it, which, being free of sulfur and nitrogen, would allow us to obtain biodiesel that, via combustion, will not emit SO<sub>x</sub> or NO<sub>x</sub> (Tamás et al., 2020).

In conclusion, by using paraffins, such as nonane and those obtained in the oligomerization of it in the diesel fuel mixture, a fuel with a higher number of cetane will be obtained that would comply with the standards of the European fuel quality directive, minimizing the emission of greenhouse gases.

### 1.2.3. Nonenes for gasoline blending

Gasolines are basically composed of alkanes (paraffins), alkenes (olefins) and aromatics. To measure the performance of this, it is done by the octane number, where the higher its value, the greater the efficiency of the engine obtaining a complete combustion. Furthermore, this lessens harmful emissions, reducing the effects on health and the environment.

Olefins are the main contributors to the number of octane in gasoline. Gasoline is normally composed of olefins with a lower number of carbonates (C<sub>5</sub>-C<sub>7</sub>) and branched olefins, known as i-olefins, because of their higher-octane number.

Given the demand for a fuel with a lower environmental impact, new regulations are implemented that aim at a drastic reduction in sulfur emissions by imposing a very low concentration of this element in fuels. For this reason, gasoline must undergo a cleaning treatment. The most used technology for this treatment is hydrodesulfurization (HDS), since it removes sulfur at a low additional cost.

When carrying out the HDS process, an octane loss is observed and therefore the yield of the final product is reduced compared to its initial state. That is why studies have been carried out to minimize this negative effect, where it is concluded that the loss caused by hydrodesulfurization can be compensated by adding olefins with a low octane number in gasoline, as commented by Dong et al., 2018.

The influence of the hydrogenation of different olefins on the loss of octane number during HDS was investigated according to the different properties of the olefins and as a function of the amount of saturation of these.

For the different properties of olefins, it was concluded that:

- The lower the number of carbons in the olefin, the greater the negative effect. Obtaining the following order from highest to lowest negative effect: C5, C6 > C7 > C8 > C9 > C10.
- Branched olefins were less negatively affected than the linear ones.

Finally, regarding saturation, the study concludes that the higher the degree of saturation, the greater the loss of octane during hydrodesulfurization. This is because olefins are more difficult to hydrogenate, they offer a greater aesthetic impediment. The degree of saturation decreases as the carbon number increases and therefore C5-C7 olefins have a greater negative effect on the loss of octane number during the hydrodesulfurization process compared to C8+ olefins.

In conclusion, using C5-C7 olefins in the fuel provides a higher octane number and therefore a fuel with a higher performance. However, gasoline must be cleaned to eliminate the sulfur content through a dehydrosulfurization process, where we can observe a decrease in the octane number from what was obtained initially. For this reason, the use of nonenes (C9) in a mixture of gasoline with C5-C7 olefins, despite having a low octane number, will allow to counteract the negative effect of hydrodesulfurization due to the effects discussed above, while achieving a balance and getting less octane loss in the process. Furthermore, since nonenes come from biomass resources, it generates bioenergy through a net carbon balance keeping it benign for the environment (Dong et al., 2018).

### 1.3. CATALYSIS

Considering the phase in which the catalyst and the reactants are, catalysis is classified as:

**Homogenous:** The catalyst is on the same phase of one of the reactants. This type of catalysis has high selectivity and yield on the desired product. Despite these advantages they present some drawbacks in the conditions of temperature and pressure, problems for the separation and recovery of the catalyst, corrosion for equipment, and the toxicity to humans. Due to these problems, this type of catalysis has a high production cost and are not ecofriendly (Izquierdo et al., 2004; Li et al., 2013).

**Heterogeneous:** The catalyst and the reactants are not in the same phase. The most common one is the use of a solid catalyst. They are easier to be separated from final products, since we are splitting two different phases (solid and liquid). They also have a better recycling performance and low corrosion, solving the problem that we had in the homogeneous route (Li et al., 2013; Trombettoni et al., 2018). However, the presence of a solid structure can affect the

reaction rate, as it includes the limitation of transfer between phases, conditioning the accessibility of the reactants to the active centers. (Izquierdo et al., 2004; Li et al., 2013).

The use of homogeneous catalysis within the industry has been reduced to 10-15%, considering heterogeneous catalysis as a better option as is cheaper and does not cause corrosion (Ramírez et al., 2017).

For a solid to act as a catalyst, at least one of the reactants must interact with its surface to be adsorbed. Therefore, having a large surface area is essential for the reactants. Porous solids are known to feature a large surface area per mass unit. The structure of solid catalyst particles (number, size, and pore volume) is elemental for the catalyst to operate properly. Reactant adsorption, reaction and desorption are the different chemical stages of a solid catalyst particle that take place on the catalyst surface, named active center. The type of adsorption is specific for each catalyst depending on the type of catalysis reaction performed (Izquierdo et al., 2004).

Studies have been carried out with different types of acid catalyst for the dehydration of alcohols with ionic-exchange resins, zeolites, nafion and alumina (Bringué et al., 2017). Despite that nafion presented excellent results, their elevated price would affect the SGB by increasing their cost. As previously discussed, we must reduce the cost of SGB until it is compatible to the price of fossil fuels before acknowledging it as an alternative. Zeolites and alumina require both high temperatures for alcohol conversion. On the other hand, ion exchange resins have also shown good results for the dehydration of alcohols. Furthermore, they are more mechanically stable, cheaper than the others and can operate at lower temperatures (Bringué et al., 2017; C. Casas et al., 2011).

Acidic ion-exchange resins of polystyrene-divinylbenzene (PS-DVB) are insoluble polymeric structures, long hydrocarbon chains structured by a cross-linking agent, with functional groups anchored that are capable to exchange ions with the medium and can be constructed from inorganic or organic monomer units. The most studied catalytic functional group is the sulfonic acid. Acid ion exchange resins are composed by copolymers of styrene-divinylbenzene of two morphologies and sulfonic acid groups ( $-\text{SO}_3\text{H}$ ) as functional, attached on to the preformed Crosslinked polymeric matrix. For this reason, these resins can be used as catalysts for dehydration of alcohols to olefins or ethers by the process showed in the Figure 6.



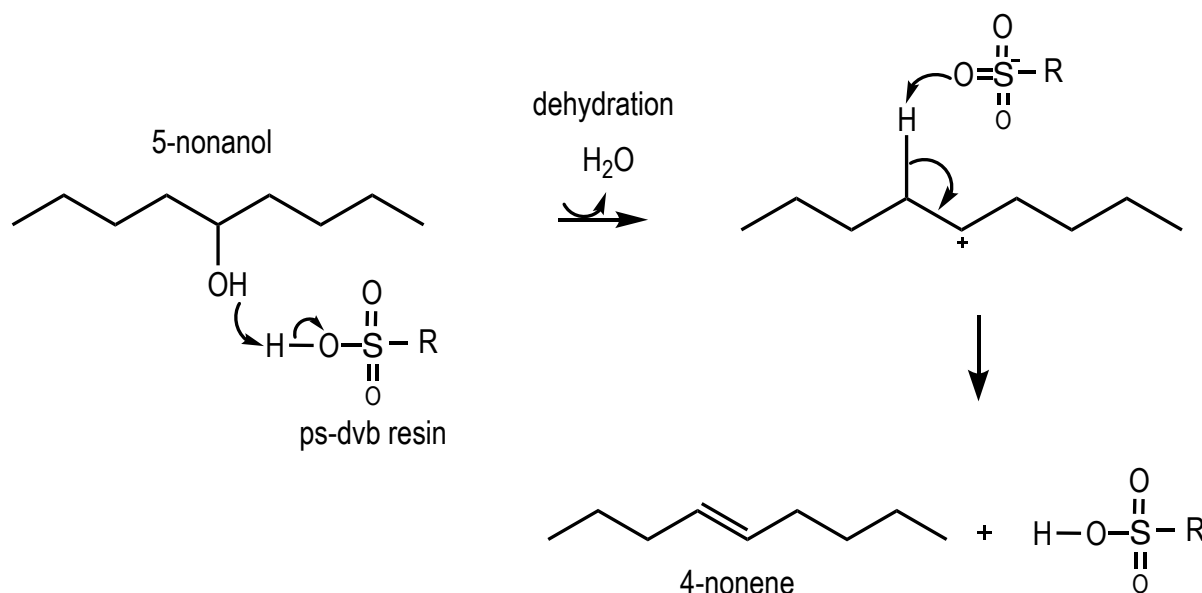


Fig 6. Dehydration of 5-nonanol with acidic ion-exchange resins of polystyrene-divinylbenzene.

The effectiveness of each catalyst is influenced by the level of crosslinking controlling resin porosity, particle diameter, swelling capacity (this is fundamental to control substrate accessibility), size of the reagents and products, acid capacity (number of accessible sulfonic groups in a completely swollen state), density, nature of the polymer, affinity of water and its stability (Tejero et al., 2016).

Therefore, there are different types of morphological structures:

### Gel-type:

This type of acidic ion-exchange resin can have a quasi-homogeneous behaviour in an aqueous medium and have a translucent polymeric homogeneous matrix structure inside the beads. They have a microporous structure and a lower percentage of crosslinking that allows accommodating large molecules making them soft, elastic and mechanically unstable resins. They consist of two types of pores: micropores for the inaccessible part of the matrix and accessible mesopores formed in the swelling. Therefore, the pore structure is not permanent, and it depends on the medium. In a nonaqueous medium, the matrix is completely impermeable so there is lower catalytic activity because there is only access to the available active centres on the surface of the beads. However, if we work within an aqueous or strongly polar medium, the polymer chains separate due to swelling and therefore access to the functional groups is facilitated. To summarize, gel-type resins should be used in a swelling medium capable of expanding the polymeric matrix, obtaining access to all of its active centre (Ramírez et al., 2017).

To solve this problem, it was decided to give a certain rigidity to the polymeric structure with chains linked together by means of divinylbenzene, thus obtaining the macroreticular resins (Bingué et al., 2013).

### **Macroreticular resins:**

These are the most widely used materials, with an opaque and rigid polymeric heterogeneous matrix structure. They are composed of three types of pores: the micropores which are present in the inaccessible zone when the molecule is not embedded in the polymeric matrix, mesopores and macropores of permanent porosity. In a non-aqueous medium, they have a high porosity and surface area, to help maintain accessibility to acid groups. Therefore, the catalytic activity of macroreticular resins is effective in both mediums, aqueous (strongly polar) and in nonaqueous (apolar) (Ramírez et al., 2017; Tejero et al., 2016). In a non-aqueous medium, they have a high porosity and surface area, to help maintain accessibility to acid groups. They are harder and more resistant due to the higher percentage of cross-linked with a larger surface area than gel-type. Despite this, they can be fragile and because of their high degree of crosslinking leads to internal mass transfer problems, involving lower activities due to the difficulty in reaching active sites and have a lower thermal stability. Being thermostable allows a resin to withstand higher temperatures. In general, gel type resins show more thermal stability and can work till 150°C. The solution to the lower thermal stability involves the addition of electron donating groups substituting hydrogen atoms in polymer chains. A clear effect of this improvement is the Amberlyst 45 macro resin, it has chlorine atoms in its structure, which confer a higher thermal stability and can work up to a maximum operating temperature of 190°C (Ramírez et al., 2017).

## **1.4. STATE OF THE ART OF NONENES PRODUCTION BY ALCOHOL DEHYDRATION**

Through an analysis of studies with similar alcohol dehydration reactions using the same catalyst, the presence of two types of reactions was observed, towards the formation of olefins and to obtain linear ethers, as in the case of dehydration of 1-octanol. These reactions could be observed in the present study.

Eventually, this study is based on the pre-existing data made by Alonso et al., 2010, where the dehydration of the 5-nonanol reaction with different resins is studied. As a result, the silica-alumina catalyst showed no catalytic activity, while the H-ZSM5 zeolite and sulfated zirconia

showed very low activity but measurable. Nafion SAC 13 and Amberlyst-45 showed higher catalytic activities, achieving conversions of 38% and 43%, respectively, after a reaction time of 4 h at 433 K.

To summarize, it can be seen that catalysis by ion exchange resins of PS-DVB presents high conversion values for this reaction. It would be interesting to expand this research and determine what type of resin would offer the most promising and optimal working conditions for the obtention of olefins (nonenes).

## 2. OBJECTIVES

The goal of the present study is to expand the pre-existing data for the dehydration of 5-nonanol by ion exchange resins of PS-DVB. It is proposed to perform a resin screening and find the most suitable operating conditions to maximize nonene production.

This study has been designed to:

1. Determine which types of resins will be most suitable for this reaction, comparing the conversion, reaction rate and selectivity of the different catalysts at a constant temperature.
2. Deduce which resin properties have the greatest influence on catalyst activity under the experimental conditions.
3. Test the reaction at different temperatures with Amberlyst 45.
4. Finally, evaluate the apparent activation energy of the reaction.

### 3. EXPERIMENTAL SECTION

Experiments for the synthesis of nonenes were carried out using 5-nonanol with a purity of  $\geq 95\%$  (MERCK, Code: 29051900) as reactive. Dioxane with a purity of  $\geq 99.5\%$  (FISHER, United States) was used as solvent to prevent the formation of different phases, the three-phase diagram (Figure 7) shows the formation of 2 phases with even low concentrations of water.

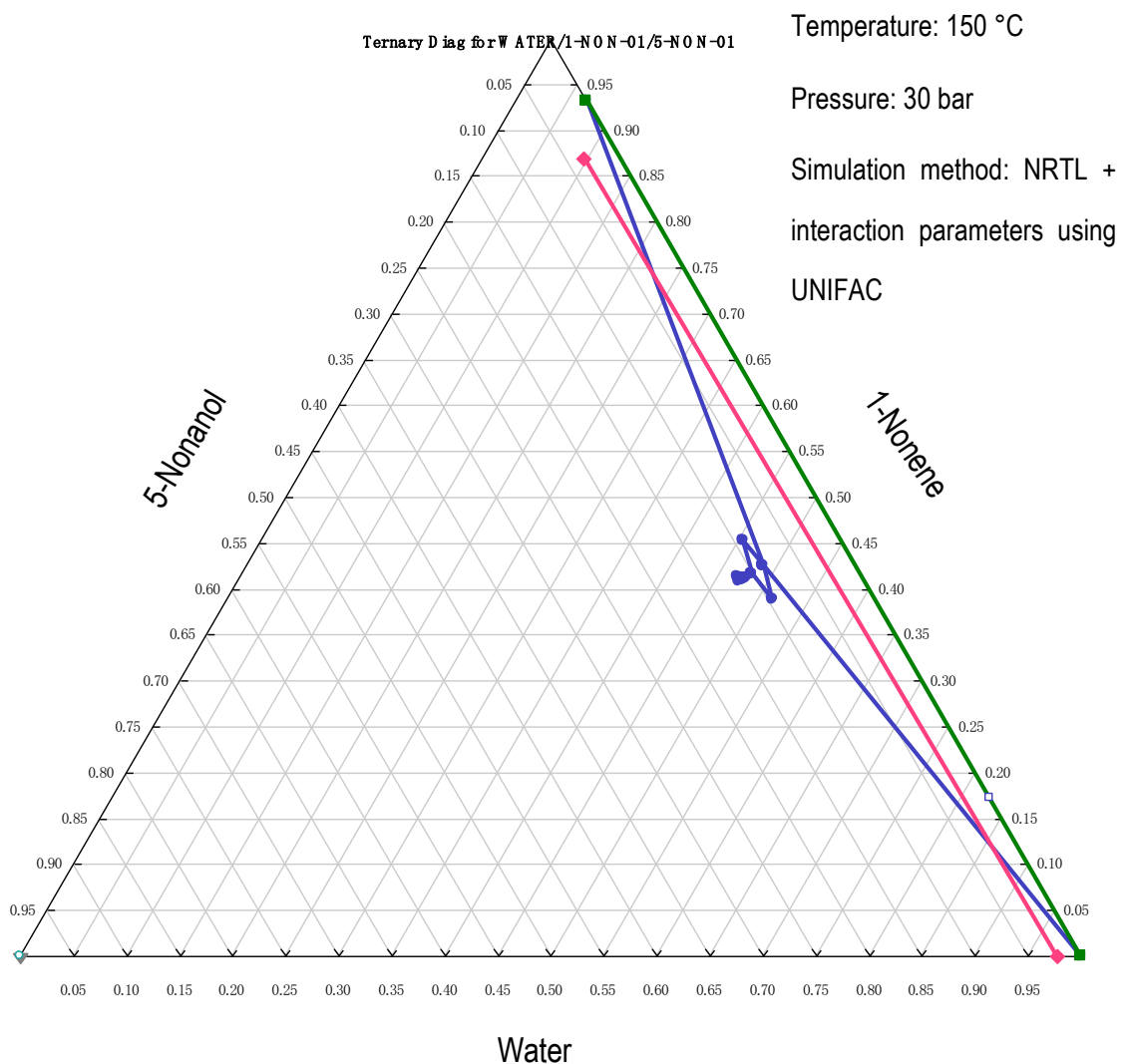





Fig 7. Three-phase diagram Water/5-Nonanol/1-Nonene

Each component relative properties are shown in Table 3.

Table 3. Relevant properties of the different components.

PROPIERTIES	5-NONANOL	DIOXANE	4-NONENE
CAS number	623-93-8	123-91-1	2198-23-4
Molecular mass (g/mol)	144.26	88.106	126.24
Density (kg/m <sup>3</sup> )	821	1033	743
Melting point (°C)	-5.0	11.8	Not available
Boiling point (°C, at 760 mmHg)	213	101.1	145.7
Flammable Limits	Not available	22%(v) 25%(v)	3,9%(v) 0,7%(v)
Hazard information	 Irritant	 Health Hazard Irritant Flammable	 Flammable Health Hazard

The nitrogen gas, with a purity of 99.9995%, is used for the pressurization of the reaction at an overpressure of 30 atm. The helium with a purity of 99.998% is used in the chromatographic technique as a carrier gas.

Ion-exchange polystyrene-divinylbenzene (PS-DVB) sulfonated resins (see Table 4) were used as catalysts.

Table 4. Characteristics and structural parameters of resins in dry state and swollen in water

Type	Catalyst	Sulfonation type <sup>a</sup>	T <sub>max</sub> <sup>c</sup> [°C]	[H <sup>+</sup> ] <sup>b</sup> (mmol/g)	DVB %	d <sub>p</sub> <sup>c</sup> (mm)	Water retention <sup>c</sup> (%)	d <sub>pore</sub> <sup>d</sup> (nm)	ΣV <sub>pore</sub> <sup>d</sup> (cm <sup>3</sup> /g)	ΣS <sub>pore</sub> <sup>d</sup> (m <sup>2</sup> /g)	ΣV <sub>sp</sub> <sup>e</sup> (cm <sup>3</sup> /g)
Macroterricular	A-35	OS	150	5.32	20	0.51	51-57	12.6	0.72	199	0.50
Macroterricular	A-45	MS	190	2.65	8	0.57	53-59	13.2	0.22	66	1.15
Gel	DOW50Wx2	MS	150	4.83	2	0.50	74-82	---	---	---	2.68

(a) Monosulfonate (MS), Oversulfonated (OS).

(b) Titration against standard base.<sup>1</sup>

(c) Manufacturer data.

(d) Swollen state (in water)

(e) Specific volume of swollen polymer in water, measured by ISEC technique

### 3.1 EXPERIMENTAL SETUP

The experimental set up, as can be seen in Figure 8, consists of a 100 mL stainless steel batch reactor (316 SS Autoclave Engineers), an electrical heating system which includes a thermocouple for the control of the external wall reactor temperature, two control systems one for the stirring speed through a frequency converter and the other one as control of the temperature system with an error margin of  $\pm 0,1^{\circ}\text{C}$  and finally a gas chromatography for the analysis of aliquots.

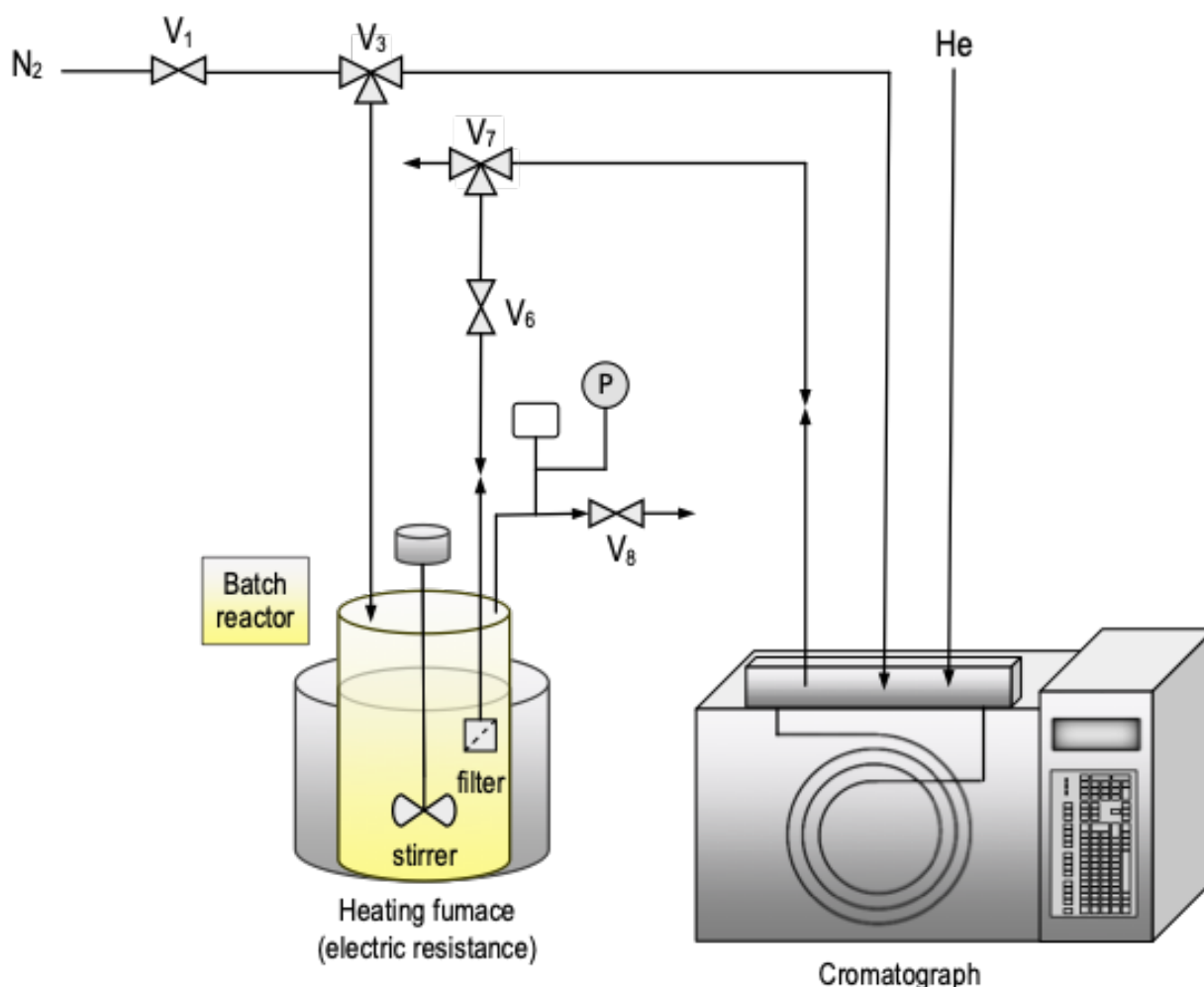


Fig 8. Experimental setup

In addition, the reactor is equipped with a stirring, a relief valve, a pressure meter, a thermocouple, a baffle plate and a rupture disc.

The baffle plate is made of stainless steel and placed close to the walls of the reactor used to avoid the formation of a vortex and allowing it to work in optimal agitation conditions.



A relief valve is placed for reactor depressurization that can also be used in case of unpredictable overpressures, with a rupture disc that can withstand a maximum pressure between 50.1 and 54.8 bar with an error margin of 5%.

The reactor has two inlets, one for supplying N<sub>2</sub> gas, which is used to pressurize the reactor and the other for sampling, where part of the reactor blend is removed and returned through a mesh size porous iron filter, 5 µm. The line connecting the reactor to the analysed system must be maintained at a temperature similar to the internal mixture of the reactor using a mantle as thermal insulation. The system is analysed using a thermal conductivity detector (TCD) on a gas chromatograph.

### 3.1.1. Analytical system

Gas chromatography is a separation method used to identify and quantify volatile substances in gas phase. The basic gas chromatograph consists of an injector, a carrier gas supply, a capillary column, an oven, a detector and a data system.

The data system shows different peaks, one for each component of the reaction (see Figure 9). Furthermore, an analysis of the sample was carried out using a gas chromatograph coupled with a mass spectrometry detector to identify the exanimated substance where a formation of 4-nonene and its isomer was observed.

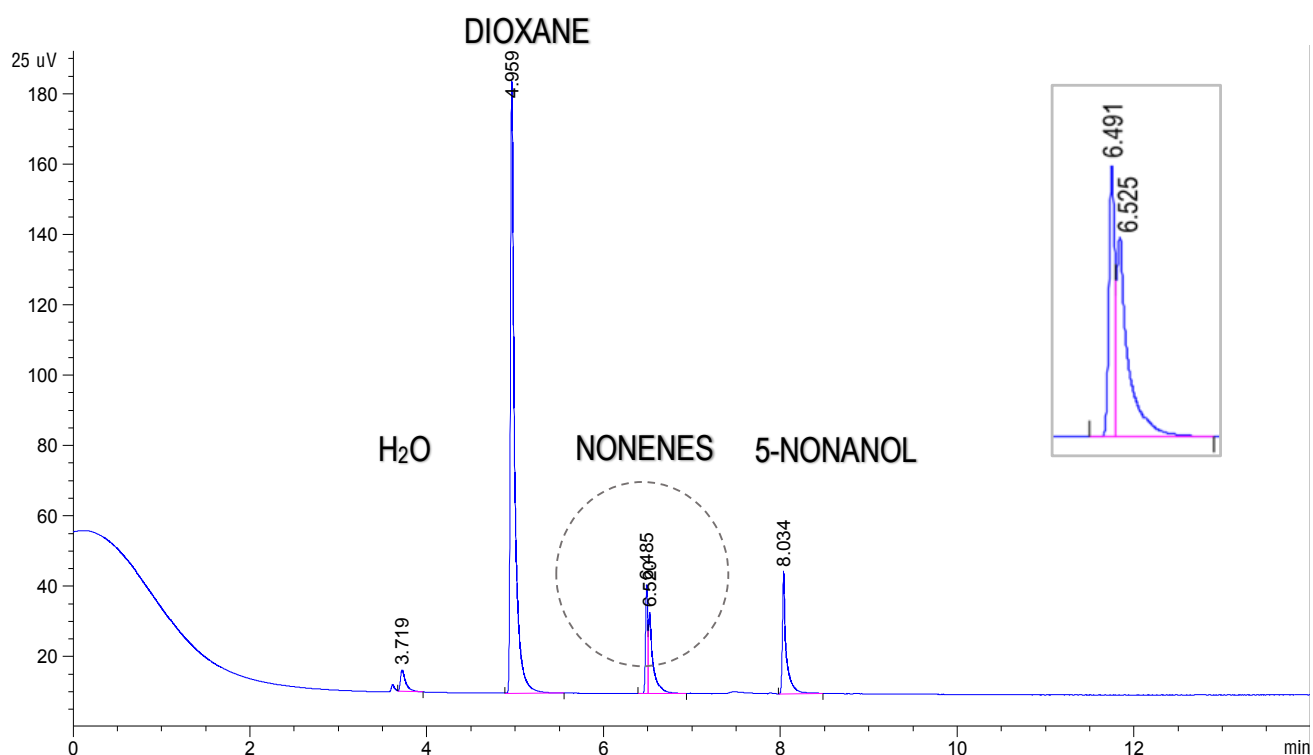


Fig 9. Gas chromatography analysis of reaction sample (150°C A45 1g).

The operation of the gas chromatograph is described below. The carrier gas flows through the preheated inlet and a small amount of the sample is injected ( $0,2 \mu\text{L}$ ), this injection is carried out with an automatically actioned valve using synthetic air. The system is heated to a high temperature to vaporize the sample. The vaporized sample is transported by carrier gas into the capillary column with the following characteristics,  $20 \mu\text{m}$  internal diameter,  $0.5 \mu\text{m}$  stationary phase thickness and  $50 \text{ m}$  long. Separation of the individual components takes place in it. The column is placed in a thermal controlled oven, so that the components remain in vapor form. After the separation, the carrier gas and the bands of the components pass through the detector and subsequently recorded within the computer data system. The detector system used is thermal conductivity detector (TCD), which compares the thermal conductivities of both gas flows, the pure carrier gas and the carrier gas plus sample components. Figure 10 shows a general scheme of the gas chromatography analysis system.

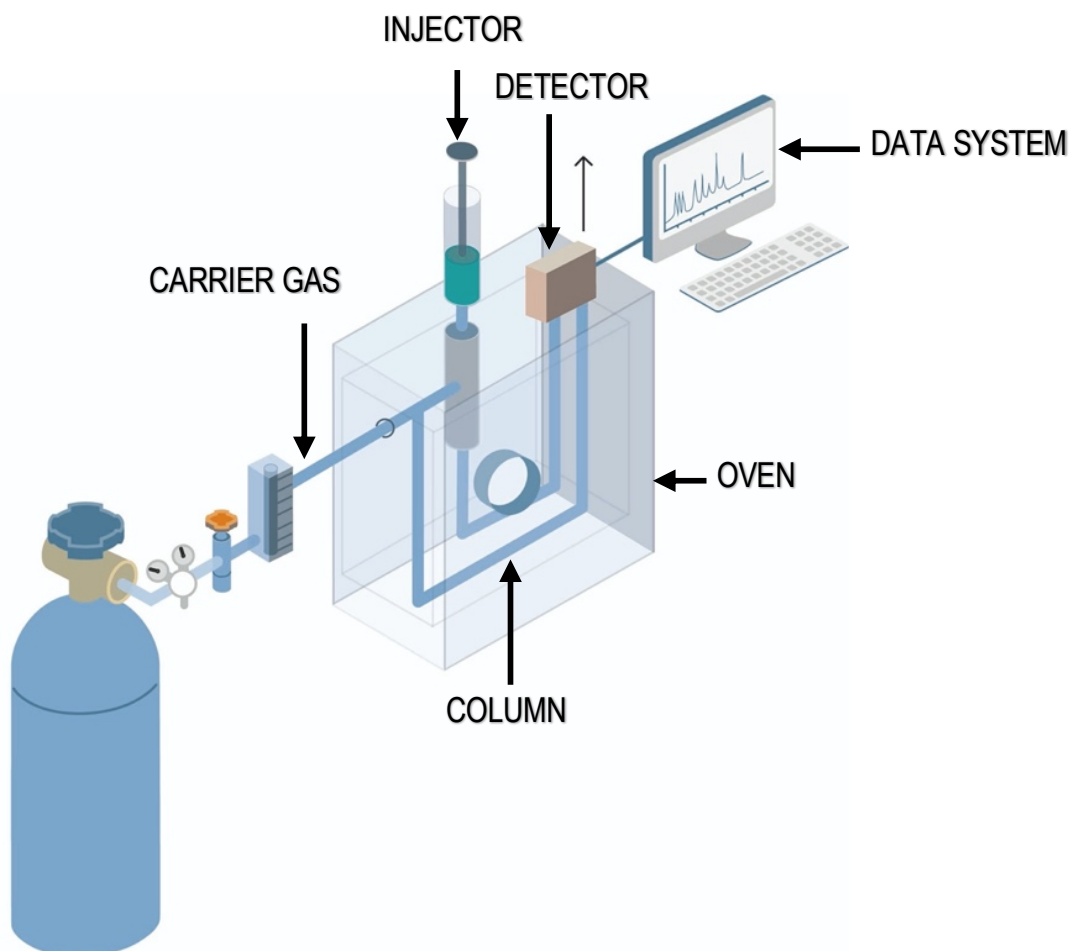


Fig 10. Scheme of Gas chromatography.

(07/06/20, via Linde company, Gas chromatography, see following link : [http://hiq.linde-gas.com/en/analytical\\_methods/gas\\_chromatography/index.html](http://hiq.linde-gas.com/en/analytical_methods/gas_chromatography/index.html) )

## 3.2 EXPERIMENTAL PROCEDURE

### 3.2.1. Resin pretreatment

The acid ionic resins must be dry before every experiment for the totally elimination of humidity. The dry process consists in two phases: first, the resins were dried overnight in an atmospheric oven at 110°C and followed by drying in a vacuum oven at 110°C at 10 mbar for a minimum of 1h.

### 3.2.2. Reactor loading

Figure 11 shows the experimental setup for this study.

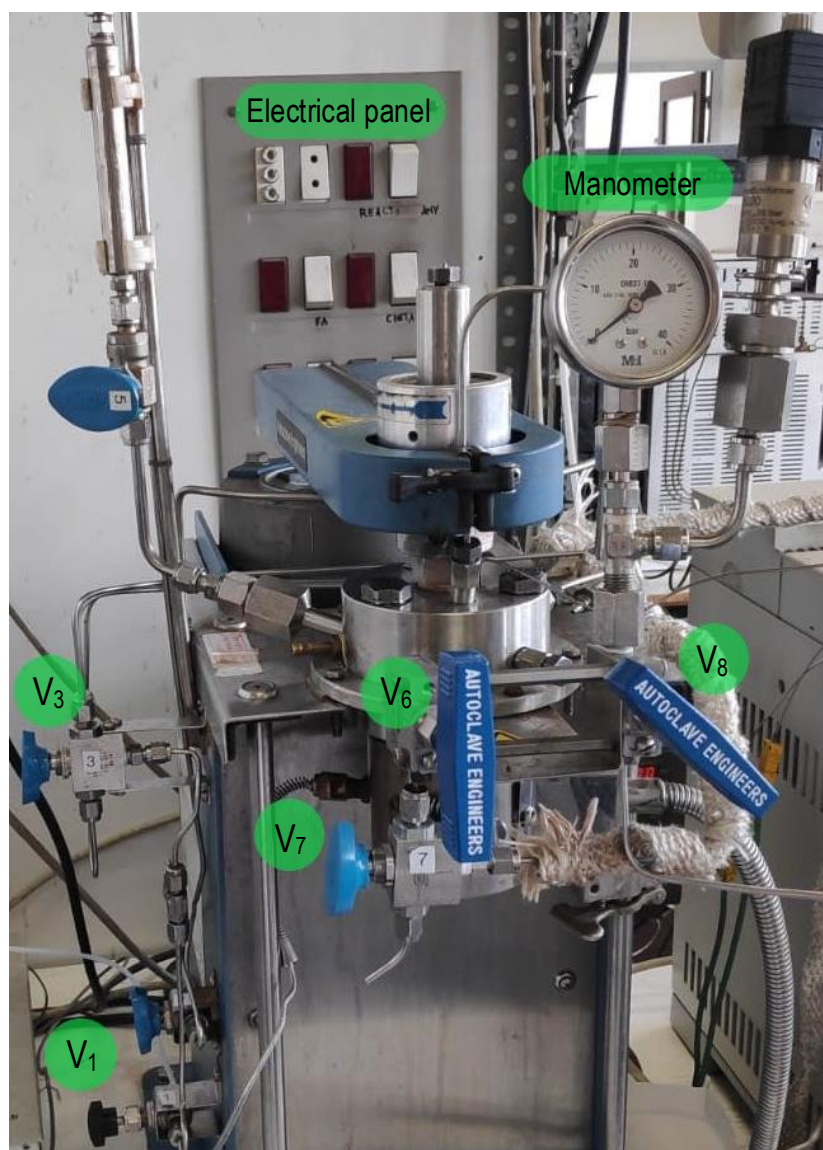


Fig 11. Assembled experimental set-up.

The reactor has a maximum capacity of 70 mL that cannot be exceeded to ensure that safety conditions are met. The feeding mixture was prepared with the dioxane, 5-nonanol and the necessary amount of resin was added for every experiment. The system is pressurized to 30 atm, and valve V1 is closed in order to observe if there is a pressure loss. If the manometer readings are not stable will indicate the presence of a leak which must be resolved in order to perform the experiment in optimal conditions. To end, the heating furnace is placed around the reactor and properly secured.

### 3.2.3. Experiment launching

When the reactor charge is complete, the next process is to turn on all the electrical components of the experiment setup. First, the agitation is set up at a speed of 500 rpm. The thermocouples of the temperature inside the reactor and its surface are programmed for each experiment, where the set point for the heating oven must be manually programmed 40°C above the operating temperature (internal temperature). Finally, the computer terminal is turned on where the program for gas chromatography analysis is loaded and the method of execution is selected.

### 3.2.4. Sampling

After the operating temperature reaches the working temperature, the first injection is made by the following steps. The valves will have to be manipulated in the following order, the V3 is switched into the position 1 so that N2 brings the sample to the chromatograph. Then, with the V7 in position 1, the V6 opens. The sample will reach the chromatograph in about a minute, at this time the analysis program is started by pressing the START button. The sample is returned to the reactor after 30 s. For reentry of the sample into the reactor, V3 is moved to position 2. The V8 is opened to cause a pressure drop of approximately 10 atm facilitating return. The V6 is closed and to purge the system, the V7 is shifted to position 2 twice with precaution to avoid micro-spraying. Finally, V3 returns to position 1 and the system is purged by opening V7 to depressurize it. The injections are repeated every hour until the end of the experiment is reached.

### 3.2.5. Clean-up

After performing the experiment, the electrical systems, agitation, and thermal system are turned off, then the GC is put into low power mode. For this, we need to access to the FRONT DETECTOR where the filament and temperature of this menu are turned off, then the GC OVEN button is pressed, where its temperature is manually adjusted to 100°C. Finally, the reactor must be depressurized by closing the V1 and opening the relief valve V8. We let the system cool down. With the system at room temperature we will remove the heating system, the screws that hold the reactor body and the reactor body. Blending product is filtered to recover its catalyst and the blend is stored. Finally, the reactor is washed, which consists of filling the reactor with deionized water and leaving it to stir for 5 minutes and then dried with synthetic air. The filter might become dirty during this process which can cause a pass resistance that will make it difficult to take the sample and return it. In that case, it is unscrewed from the support and placed in a beaker with hexane, left it 30 min in an ultrasonic bath and finally dry with synthetic air. Once completed the clean filter is screwed back on.

## 3.3. EXPERIMENTAL CONDITIONS

The experimental conditions included an experimental duration of 6 h, a stirring speed of 500 rpm, a constant alcohol to dioxane molar ratio and a pressure condition of 30 atm. This last condition is used to keep nonanol in a liquid phase with different working temperatures.

The molar ratio was calculated by the following equation:

$$R_{\frac{5\text{-nonanol}}{\text{Dioxane}}} = \frac{n_{5\text{-nonanol}}^o}{n_{\text{Dioxane}}^o} \left[ \frac{\text{mol}}{\text{mol}} \right] \quad (1)$$

Table 5 shows the different proportion of each component used and the alcohol to dioxane molar ratio value obtained.

Table 5. Alcohol to dioxane molar ratio value.

	V [mL]	m [g]	mol	R
<b>Dioxane</b>	45	45.36	0.52	0,24
<b>5-Nonanol</b>	25	19.37	0.12	

The experimental conditions for the catalyst screening are shown in Table 6.

Table 6. Experimental conditions with A35, A45 Dowex 50Wx2.

<b>Resin type</b>	A35, A45, DOW 50Wx2		
<b>P [bar]</b>	30	<b>N [rpm]</b>	500
<b>T [°C]</b>	150	<b>m cat [g]</b>	1

The determination of the optimal reaction temperature was carried out with a catalyst mass range of 1-2 g depending on the temperature. The amount of mass used was increased to be able to observe higher conversions at lower temperatures. Amberlyst 45 was used as catalyst because its thermostability allows the possibility of working with a wider range of operating temperatures from 140°C to 180°C.

The conditions for the study of the temperature effect are shown in Table 7.

Table 7. Experimental conditions with different temperatures by A45.

<b>P [bar]</b>	30	<b>N [rpm]</b>	500
<b>T [°C]</b>	140,150,160,170,180	<b>m cat [g]</b>	1-2

### 3.3.1 Other Experiments

Given the current worldwide outbreak of COVID-19, the planned study could not be completed, therefore the followings experiments reminded to be executed:

- Calibration of the gas chromatograph
- Replication of the experiment at 180°C

- Experiments using Amberlyst 35 at different temperatures
- Test at higher alcohol to dioxane ratio.

## 4. GENERAL CALCULATIONS

To compare the experiments executed with different catalyst mass the normalized time. It was calculated by the following formula:

$$t' = \frac{t \cdot w}{n^{\circ} \text{nonanol}} \left[ \frac{g \cdot h}{mol} \right] \quad (2)$$

The area% (values obtained with the chromatography system) was considered equal to the mass%, after all, the chromatography calibration was not performed.

The conversion is calculated through the moles of the reactant with the following formula:

$$X_{5\text{-Nonanol}} = \frac{n_{5\text{-Nonanol}}^{\circ} - n_{5\text{-Nonanol}}}{n_{5\text{-Nonanol}}^{\circ}} \quad (3)$$

The data system showed the formation of two nonenes. The selectivity of them is calculated to find out whether, depending on the reaction conditions, the formation of one type or the other is favored. The selectivity calculus of each nonene were achieved using the following equations:

$$S_{\text{Nonene } 1} = \frac{n_{\text{nonene } 1}}{n_{\text{nonene } 1} + n_{\text{nonene } 2}} \quad (4)$$

$$S_{\text{Nonene } 2} = \frac{n_{\text{nonene } 2}}{n_{\text{nonene } 1} + n_{\text{nonene } 2}} \quad (5)$$



In order to clearly see the difference in the relation between nonenes the following formula was used:

$$Relation_{Nonenes} = \frac{S_{nonene\ 1}}{S_{nonene\ 2}} \quad (6)$$

Since all the experiments start from the same initial condition, the reaction order was obviated. From this approximation, the reaction rate was calculated by the following equation:

$$r = - \frac{\partial n_{5-nonanol}}{\partial t} \cdot \frac{1}{w_{cat}} \quad (7)$$

The activation energy is determinate by the kinetic constant of the reaction. However, its value will be approximated as the kinetic study has not been performed. Apparent activation energy is obtained through the representation of initial velocity over different temperatures by the following equations:

$$r^{\circ} = e^{\frac{-Ea_{app}}{RT}} * A \quad (8)$$

Logarithms are applied using the following equation to linearizer:

$$\ln(r^{\circ}) = \ln A - \frac{Ea_{app}}{R} \cdot \frac{1}{T} \quad (9)$$

## 5. RESULTS AND DISCUSSION

### 5.1. REACTION ASSESSMENT

The reaction studied on the present project is show in Figure 12.

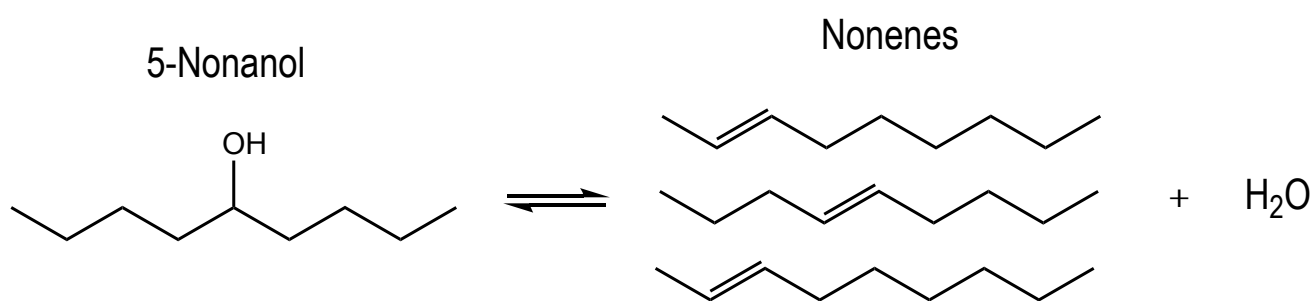


Fig 12. Dehydration of 5-nonanol.

Each experiment performs a study about the variation of the mol components over normalized time. Figure 13 shows the evolution of mol curves over time. In this Figure it can be concluded that the reactive (5-nonanol) decreases while products (nonenes) increase. The experiment results with Amberlyst 45 at 140°C are representatives for the rest of experiments.

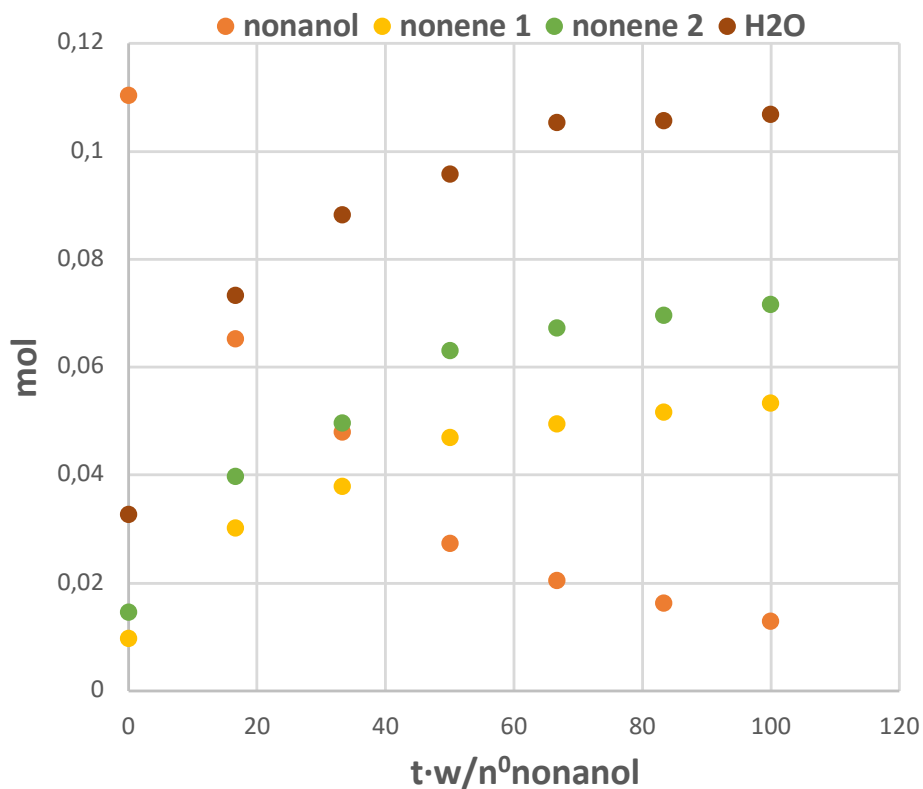


Fig 13. Mol over the course of the reaction normalized time (2g, A45, 140 °C).

The behaviour of the reaction will be determined for each study by the variation of the conversion, selectivity and reaction velocity over time or normalized time.

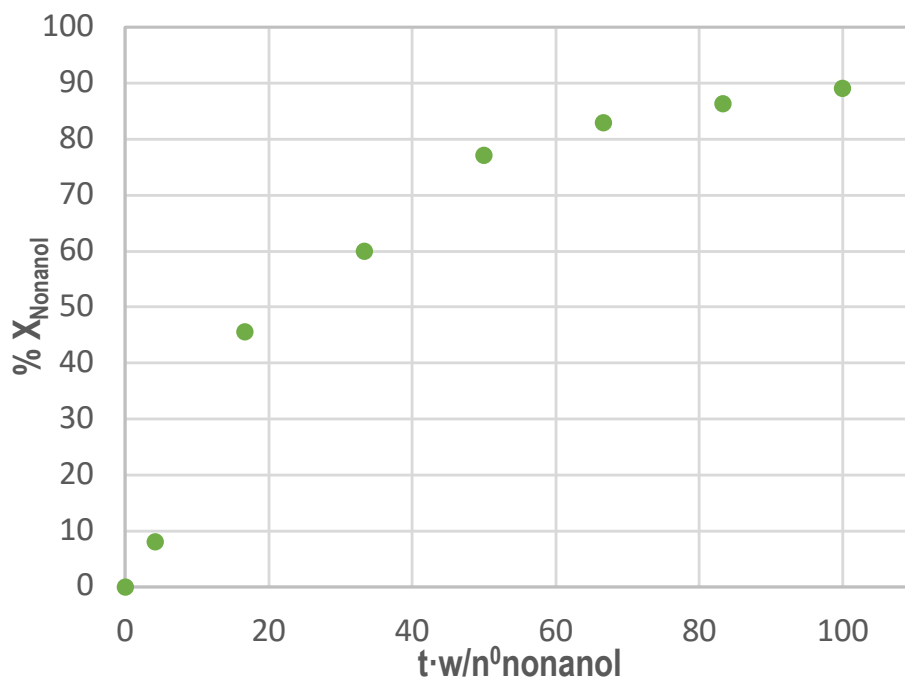


Fig 14. Conversion in front of normalized time (2g, A45, 140 °C).

Figure 14 shows the conversion over normalized time, it can be seen that the tendency of the reaction goes towards obtaining the total conversion, all the reactive is consumed.

A global selectivity study is performed to determine what conditions favour the aim reaction. The dehydration of alcohols can present esterification as a secondary reaction. However, a linear ether was not observed, obtaining a selectivity of 100% for the production of olefins (nonenes). For this reason, a study of the global selectivity was not necessary. On the other hand, a study of the individual selectivity of the nonenes will be carried out to determinate if their proportion is favoured by the different studied conditions. For each experiment the selectivity of nonene 2 was greater than nonene 1 and both remained constant over time, the balance between them was reached. Figure 15 shows the selectivity of nonenes and the relation between them over normalized time.

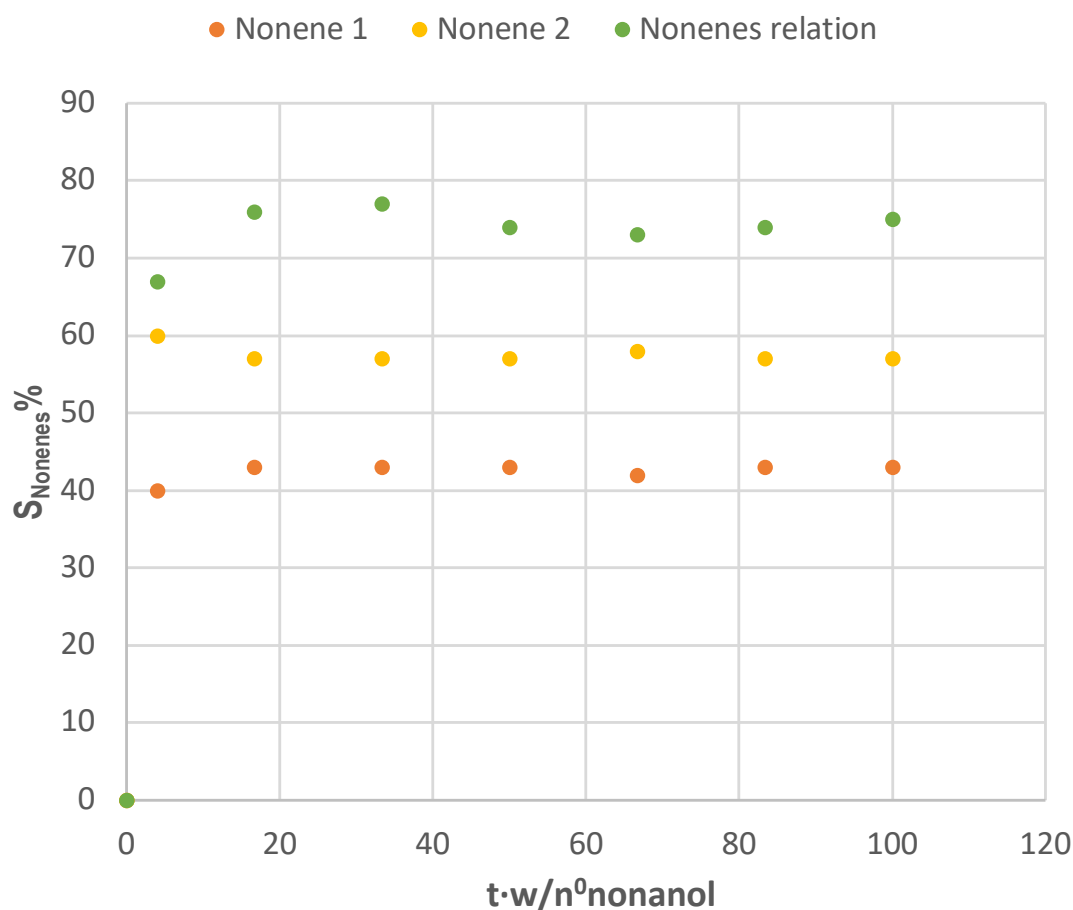


Fig 15. Nonenes relation in front normalized time (2g, A45, 140 °C).

To finalize, Figure 16 shows how the reaction velocity of the product varies over the normalized time. As was expected the reaction velocity decreases while the reactive is consumed.

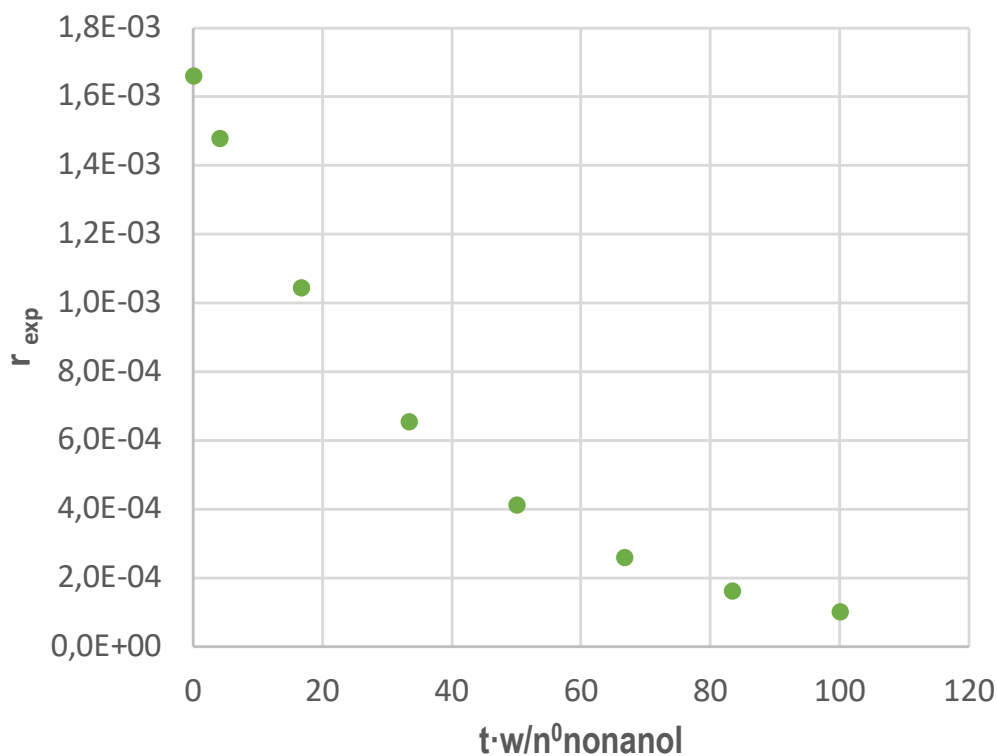


Fig 16. Reaction rate against normalized time (2g, A45, 140 °C).

### 5.1.1 Evaluation of the experimental error

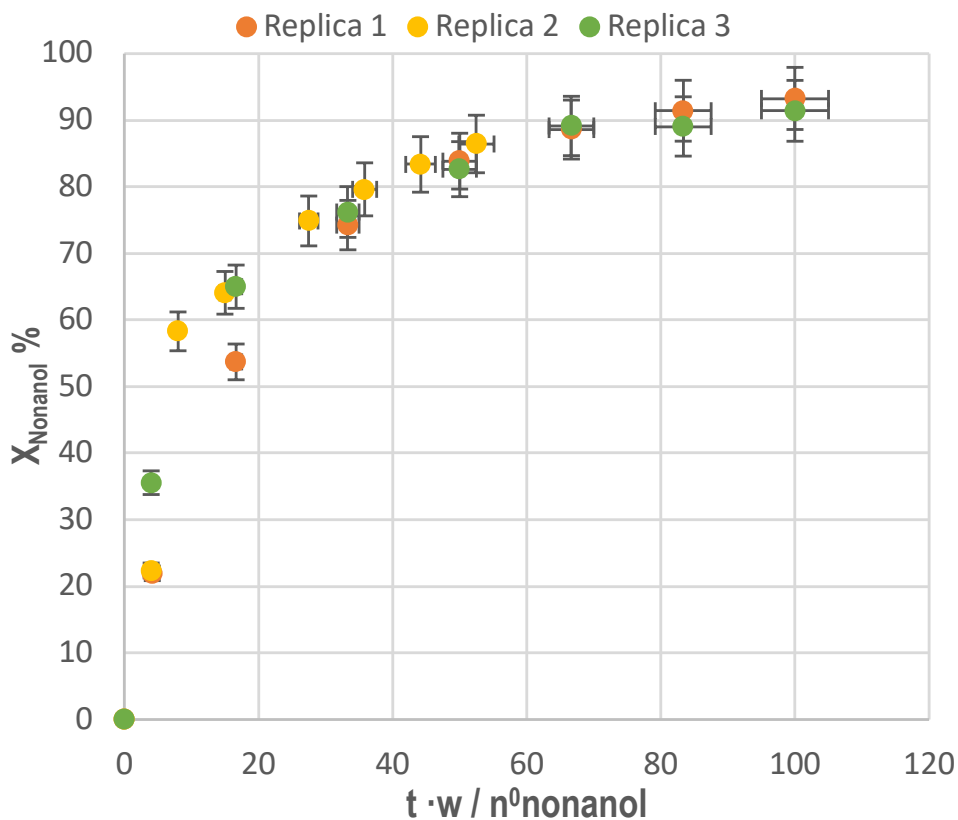


Fig 17. Replicas experiment (A45, 150 °C).

In order to study the experimental error made during the experiments, three replicas have been performed at 150°C with Amberlyst 45 as catalyst. Figure 17 shows the conversion over normalized time of the replicas. The 5-nonanol conversion obtained was of 91%  $\pm$  3%, concluding that the experiments of this study are fully replicable since the experimental error was less than 4 %.

## 5.2. EXPERIMENTAL STUDY WITH DIFFERENT RESINS

This study has attempted to ascertain which catalyst properties have a greater catalyst activity for the dehydration of 5-nonanol. The acidic resins used were Amberlyst 45 (A45), Amberlyst 35 (A35) and Dowex 50Wx2 (DOW2). Each of them, have different properties in which we can highlight:

- Different types of morphology: the macroreticular (Amberlyst 35, Amberlyst 45) and the gel type resins (Dowex 50Wx2).
- The percentage of crosslinking agent (DVB %), which provides greater or lower rigidity to the polymeric structure of the resins, differs in all of our resins (see Table 8).

Table 8. DVB % values for different resins.

Resin type	DVB%
Amberlyst 35	20
Amberlyst 45	8
Dowex 50Wx2	2

- Two different types of sulfonation, monosulfonated resins (MS) and oversulfonated resins (OS). Sulfonation influences the acid capacity and, as a general rule, the oversulfonated resins have a greater number of active sites. Table 9 shows the acid capacity of the resins.

Table 9. [H<sup>+</sup>] values for different resins.

Resin type	[H <sup>+</sup> ]
Amberlyst 35 (OS)	5.32
Amberlyst 45 (MS)	2.65
Dowex 50Wx2 (MS)	4.8

The experiments have been carried with the same mass of catalyst (1g) and same temperature conditions (150 °C). Figure 18 shows the effect of the resins over the conversion of 5-nonanol.

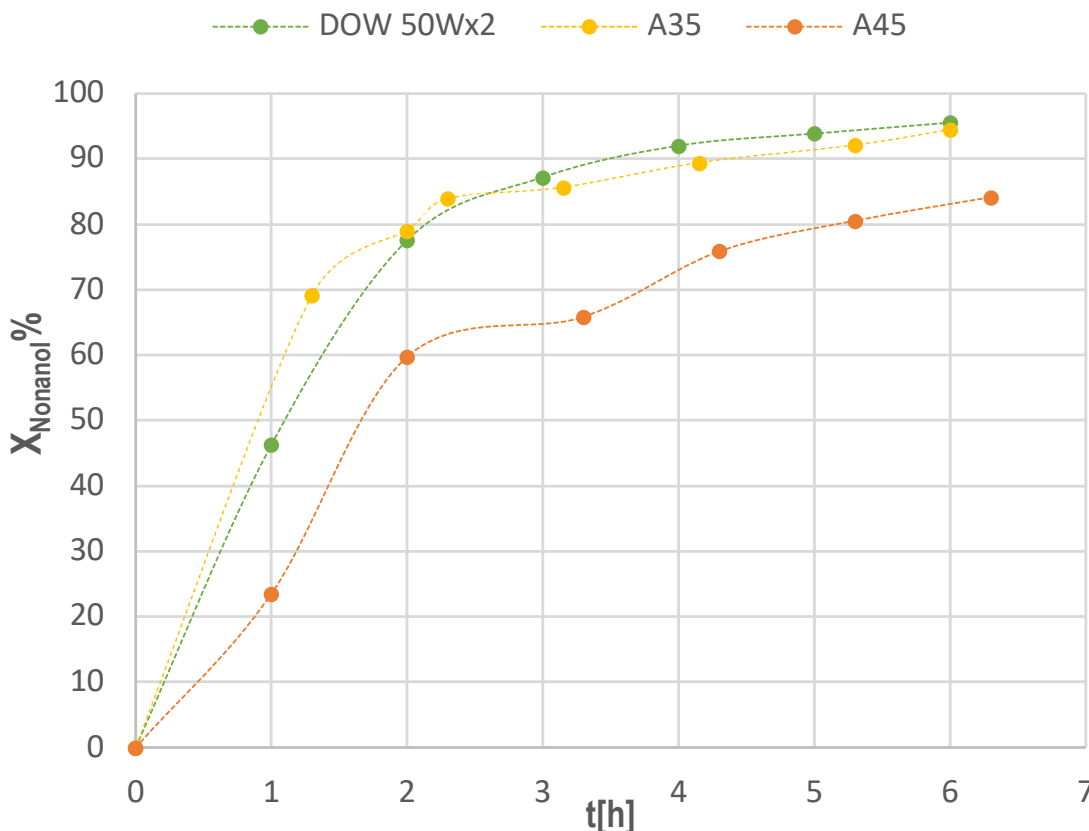


Fig 18. Conversion over time with different catalysts.

Results showed that all resins achieved high level of conversion, indicating that the acidic polymeric resins of PS-DVB are eminently suitable to catalyze for this reaction. The previous Figure showed that the best resin is Amberlyst 35 followed by Dowex 50Wx2 and finally Amberlyst 45.

Nonenes proportion can be favored between the resins used. For this reason, an analysis of its relation is performed over all the resins in Figure 19. If a difference is observed between these, the properties of the resins would affect the reaction promoting the formation of a nonene type.

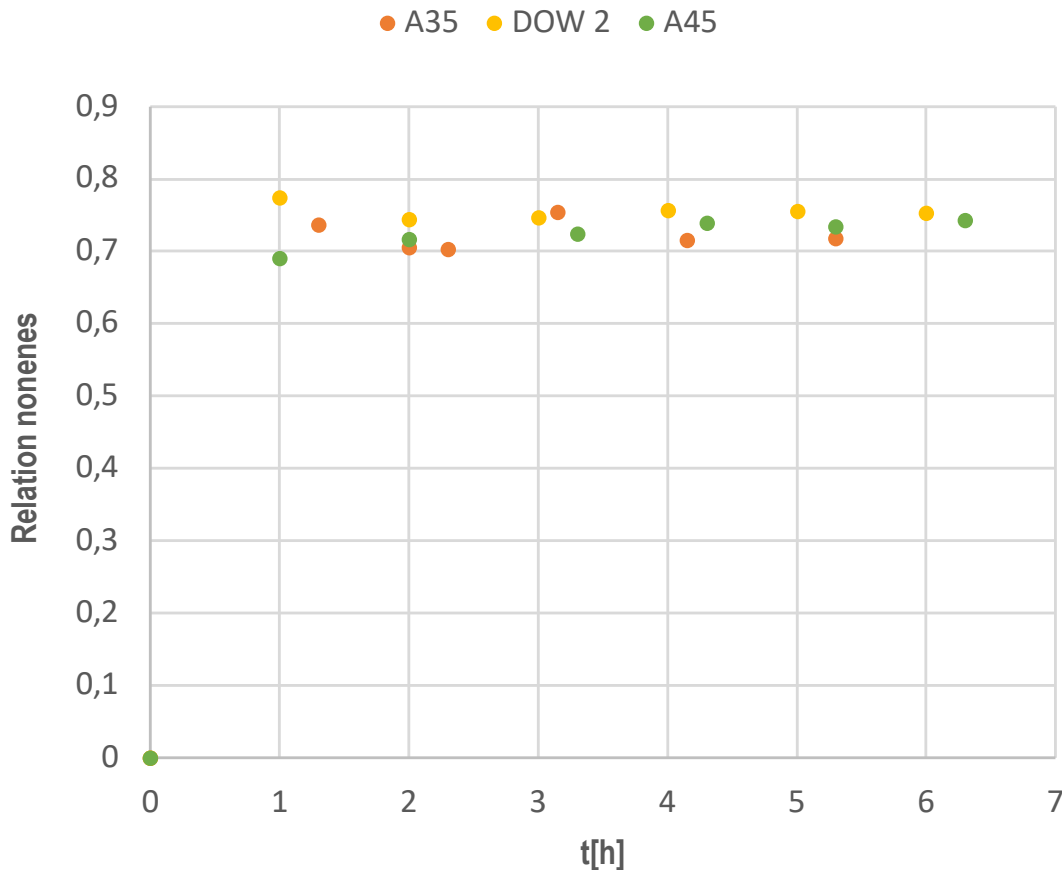


Fig 19. Nonenes relation in front of time.

Figure 19 does not show a clear variation in the relationship of the nonenes over time, the resins properties does not favor any of the nonenes.

The results are compared with bibliographic data from similar systems. Through Alonso et al. (2010) a conversion of 90% was obtained at low concentration of 5-nonanol with Amberlyst 45, a similar value is obtained of 97% applying the same conditions. Finally, the study carried out by Nel & De Klerk (2009) presented the dehydration of 1-nonanol over a fixed-bed flow reactor at 250°C using  $\eta$ -alumina as a catalyst, where the selectivity of linear ethers and nonenes was determined. Lower selectivity was obtained of 26% for the formation of nonenes and 73% for the formation of linear ethers. It is concluded that the formation of linear ethers and olefins can be observed by means of  $\eta$ -Alumina with 1-nonanol, while the ion exchange resins of PS-DVB only favoured the formation of olefins at lower temperatures by Amberlyst 45 and 5-nonanol.

To finish the study of the reaction behaviour, the effect of the reaction rate against the normalized time was analysed (Figure 20). Amberlyst 35 have the higher reaction rate compared to the others, followed by Dowex 50Wx2 and Amberlyst 45.



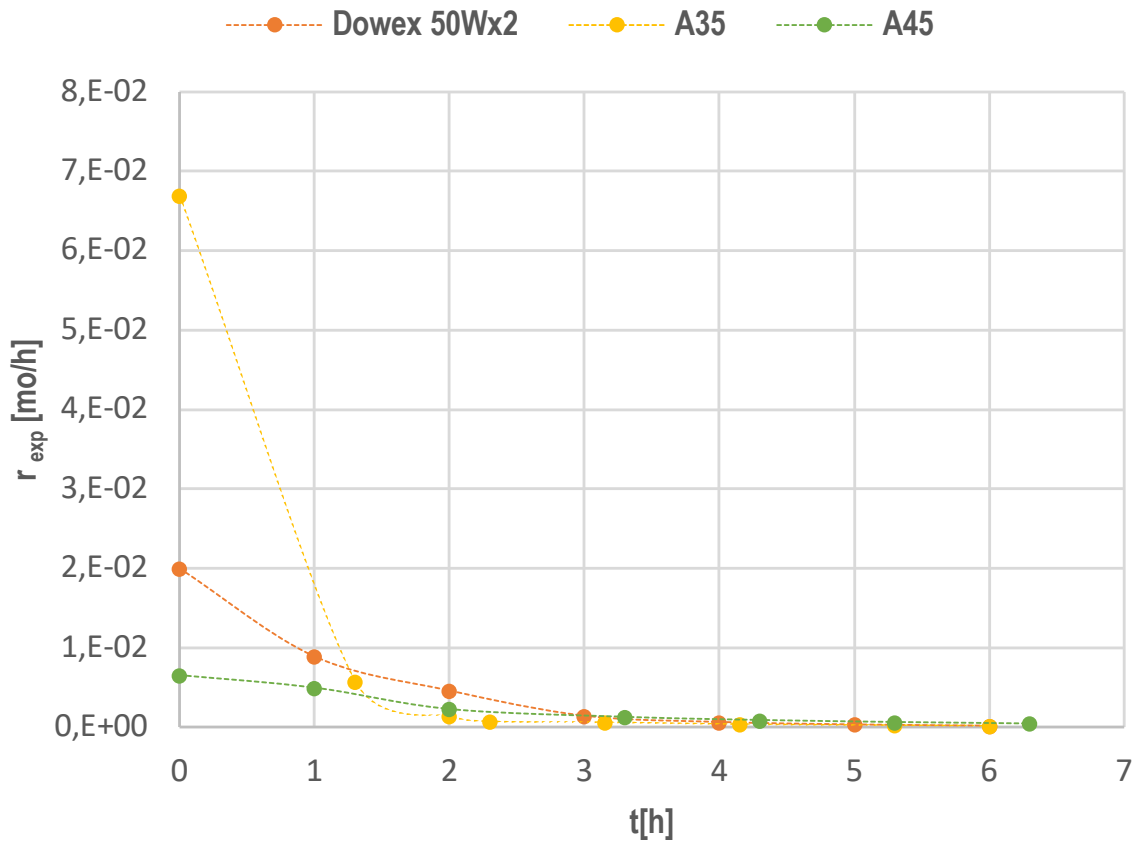
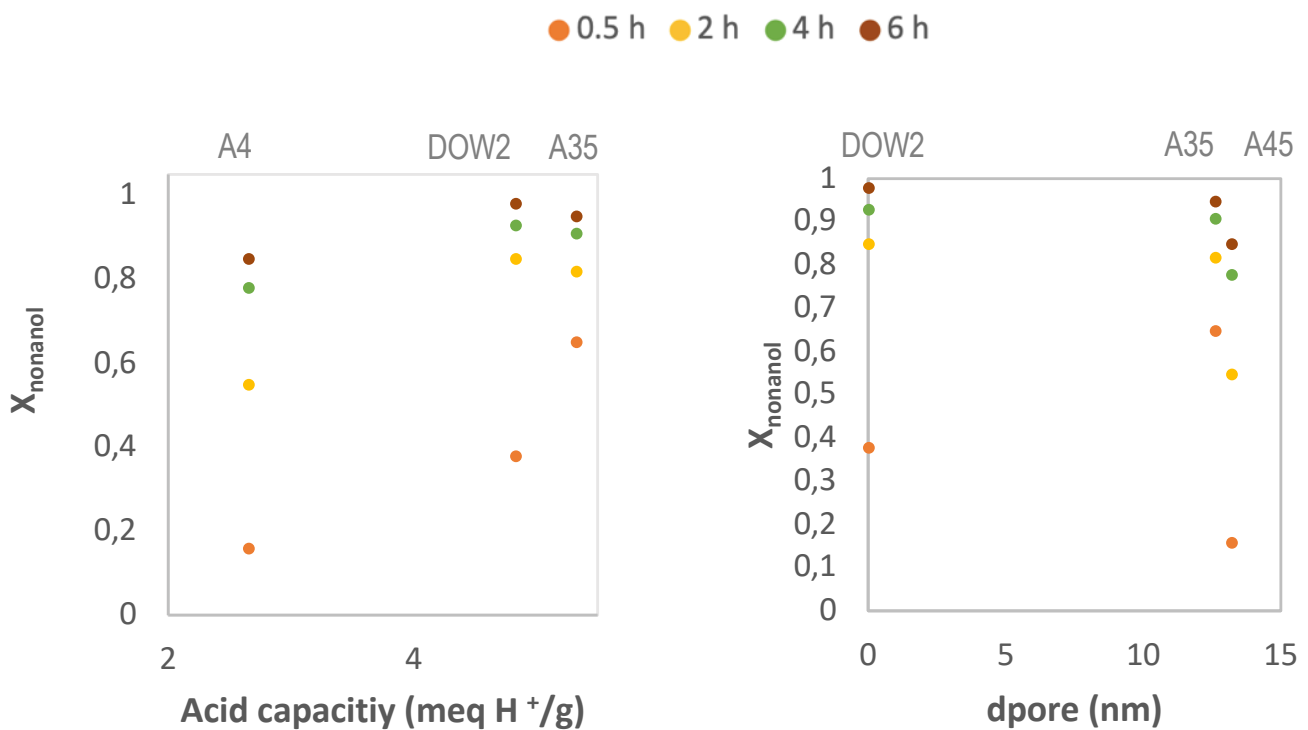


Fig 20. Velocity reaction over time.

To clearly observe which property affects the most over the course of the reaction, the different properties of PS-DVB acid resins have been related to conversion at different times as shown in Figure 21.



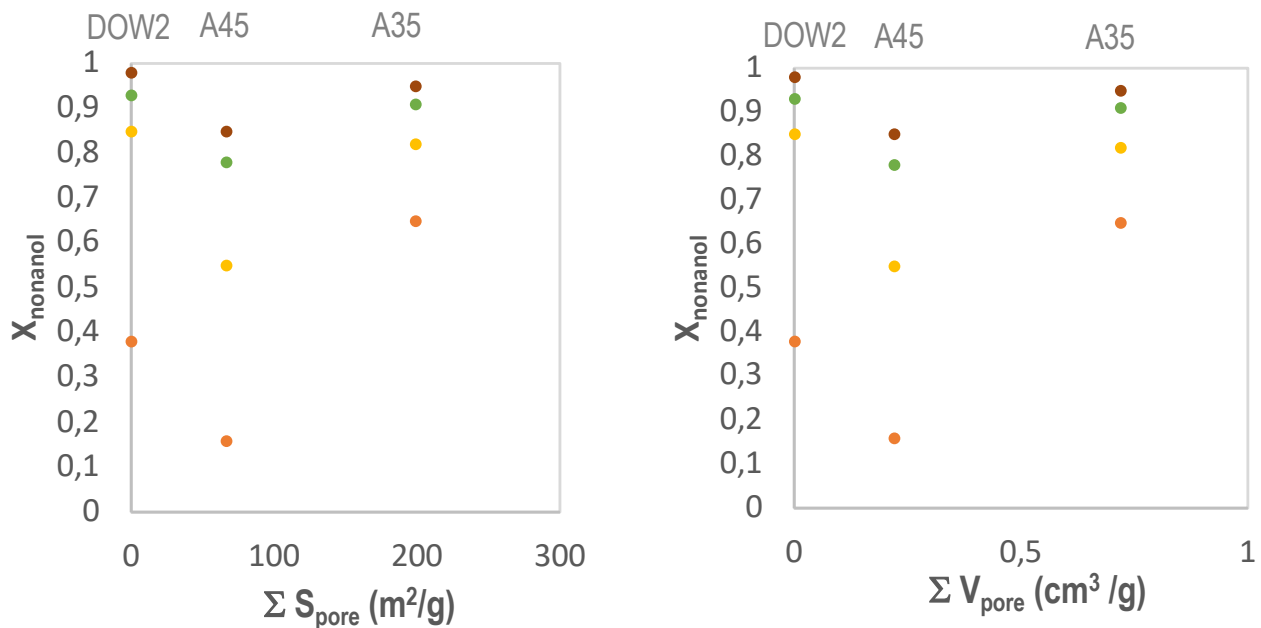


Fig 21. Conversion achieved at 0.5, 2, 4 and 6h reaction time versus acid capacity, macropore diameter ( $d_{\text{pore}}$ ), global macropore surface ( $\Sigma S_{\text{pore}}$ ).

From Figure 21 a clear effect according to the acid capacity of the resins can be seen, where a higher reaction rate will be obtained for those resins containing a greater acid capacity and therefore, a greater number of active centers. Amberlyst 35 (oversulfonated) has the highest acid capacity and, as expected, the higher conversion (65%) in a shortest period of time. In the case of the different structure properties,  $d_{\text{pore}}$ ,  $\Sigma S_{\text{pore}}$ ,  $\Sigma V_{\text{pore}}$ , no clear effect is observed between the conversion.

Working with alcohols leads to a polar medium, causing swelling in the resins especially in gel type resins (Dowex 50Wx2). The degree of swelling depends on the interaction of the catalyst with the solvent (the higher the interaction, the more swollen polymer volume) and on the degree of crosslinking (the higher the crosslinking, the less swelling). Figure 22 represents the conversion in front these parameters, the degree of crosslinking (% DVB) and the swollen polymer volume ( $V_{\text{sp}}$ ) at different reaction times.

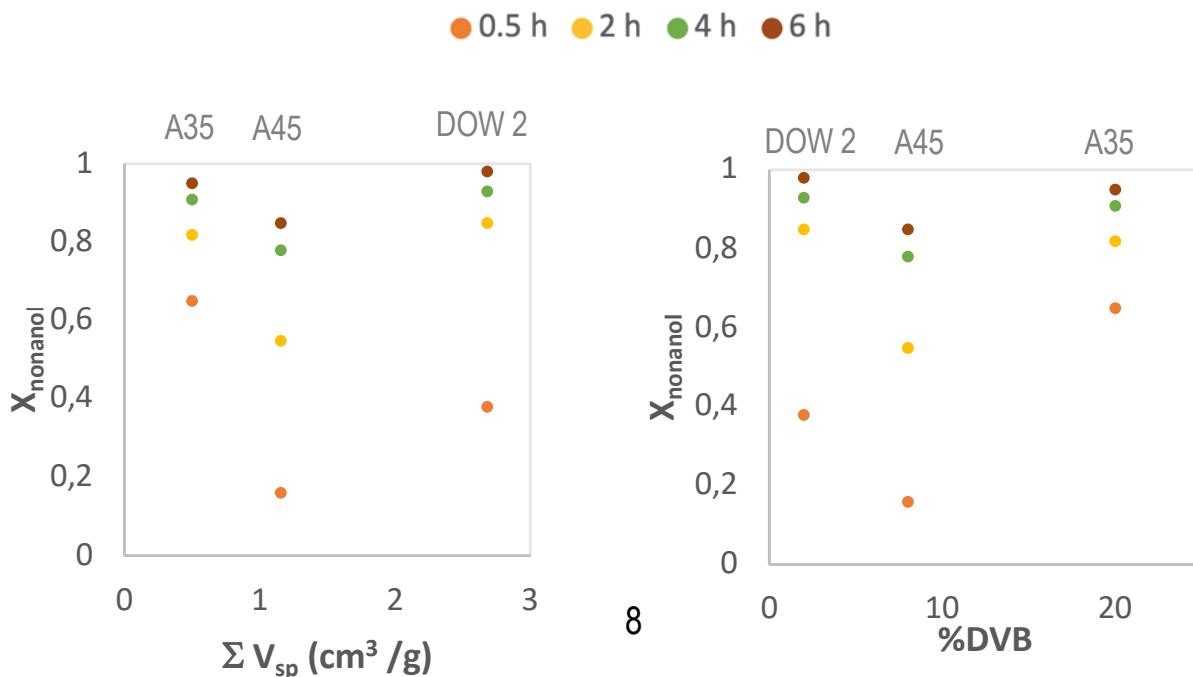


Fig 22. Conversion achieved at 0.5, 2, 4 and 6h reaction time versus specific volume of swollen polymer in water and %DVB.

From Figure 22, Dowex 50Wx2 showed the greater swelling phenomenon ( $V_{sp}$ ) due to its flexible structure (lower %DVB). This improves the accessibility to active centers through pores, allowing a final conversion equivalent to the A35. Amberlyst 35 does not have a great swelling effect due to its rigid structure, however it shows a high catalysis activity and therefore the low swelling capacity is compensated.

The modeling of the porous structure can be defined as a set of discrete fractions in which the porosity of the gel phase is described as areas of different chain density. The effect of different densities is studied with the tabulated values of the diverse densities of each resin shown in Table 10.

Table 10.  $V_{sp}$  values of the different resins.

Catalyst	$V_{sp}$ (cm <sup>3</sup> /g)				
	0.1 nm/nm <sup>3</sup>	0.2 nm/nm <sup>3</sup>	0.4 nm/nm <sup>3</sup>	0.8 nm/nm <sup>3</sup>	1.5 nm/nm <sup>3</sup>
A35	0	0	0.005	0.065	0.434
A45	0.071	0.0071	0.007	1.072	0
DOW2	0	0.729	1.949	0	0

In Figure 23 it can be seen that the difference in densities of the various resins used does not have a specific effect on the conversion as a similar degree is achieved.

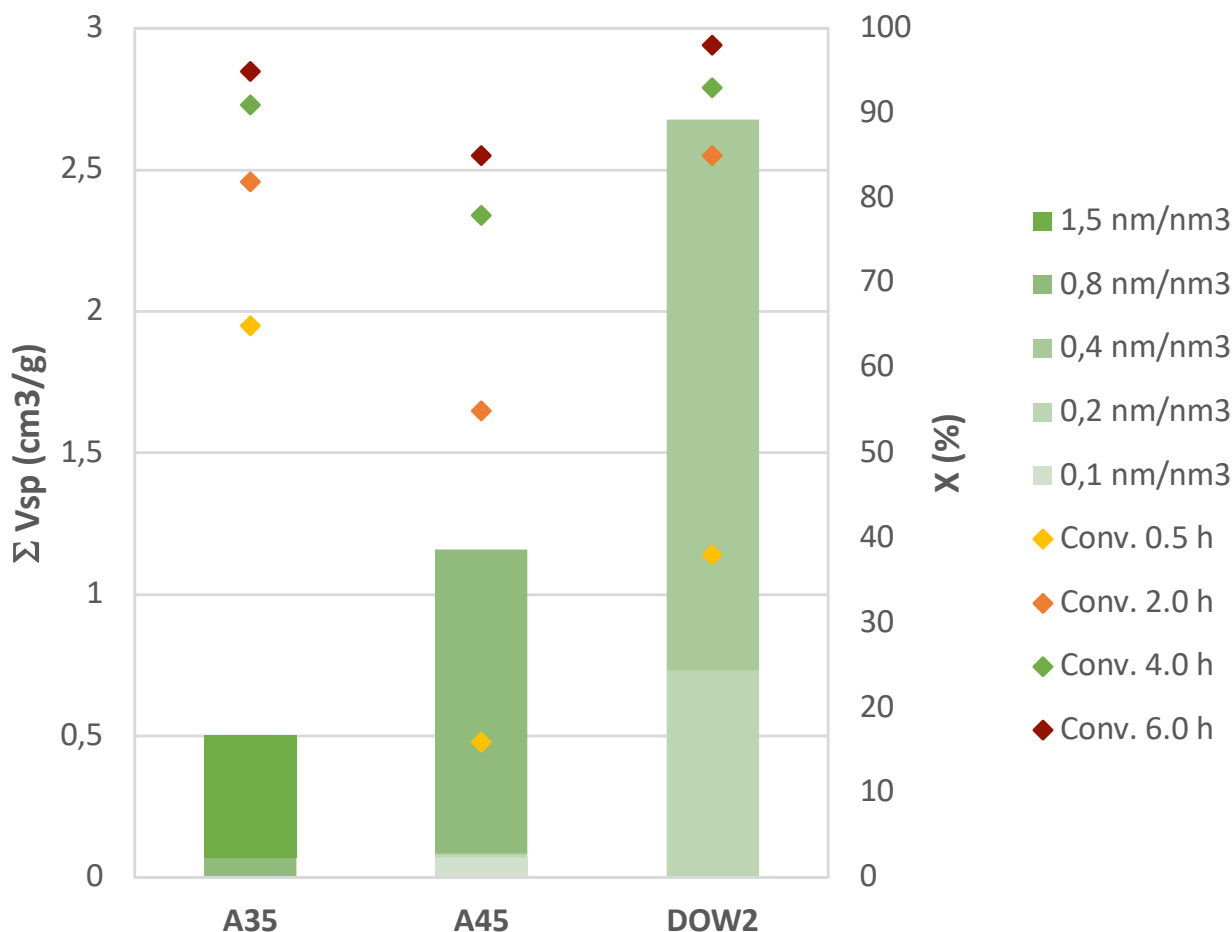


Fig 23. Densities of resins (nm / nm<sup>3</sup>) in relation to  $\Sigma V_{sp}$  and X (%).

Amberlyst 35, its oversulfonated and more rigid than the others. Its rigidity complicates the access to the pores, nevertheless it presents the highest reaction rate. It may be deduced that the catalytic activity occurs mostly on the outer surface of the catalyst. Considering 5-nonanol as a large molecule this also complicate its access through the pores to the active centres located inside the catalyst, therefore no improvement in reaction performance can be seen according to the structure of the catalyst.

Since no clear information on the catalytic behaviour is shown with separated properties, the parameter of the density of the acid sites is introduced defined by the coefficient of the acid capacity with the volume of the swollen polymer ( $[H^+]/\Sigma V_{sp}$ ). Figure 24 shows this property versus conversion.

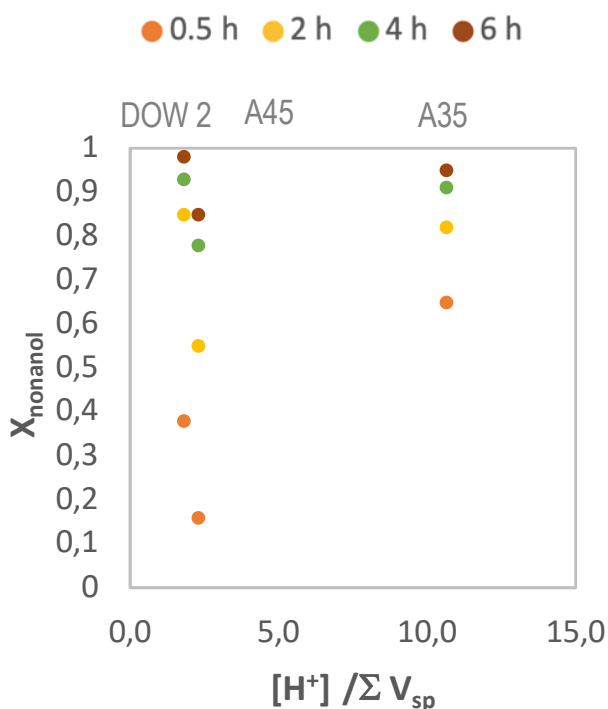


Fig 24. conversion vs density of the acid sites.

As it is demonstrated in Figure 24 the density of the acid sites does not have a clear influence on conversion.

To summarize, the study of the different structural properties of the resins showed that they do not have a direct correlation with the reaction. This is because the size of the molecule is too large complicating the access to the pores of the catalyst and therefore there is practically no internal reaction. Acid capacity was the property that showed a direct effect on the reaction behaviour. The greater the acid capacity, the greater the number of active centres, facilitating the reaction.

### 5.3. EXPERIMENTAL STUDY WITH A45 AT DIFFERENT TEMPERATURES

As previously mentioned in the article from Alonso et al., 2010, the Amberlyst 45 resin presented good conversion results for the dehydration of 5-nonanol and since is thermostable gives the possibility to work with higher temperature up to the maximum allowed of 190 °C. It was

proposed to extend this study under the effect of different operating temperatures (140-180°C). Figure 25 shows the effects on temperature over conversion.

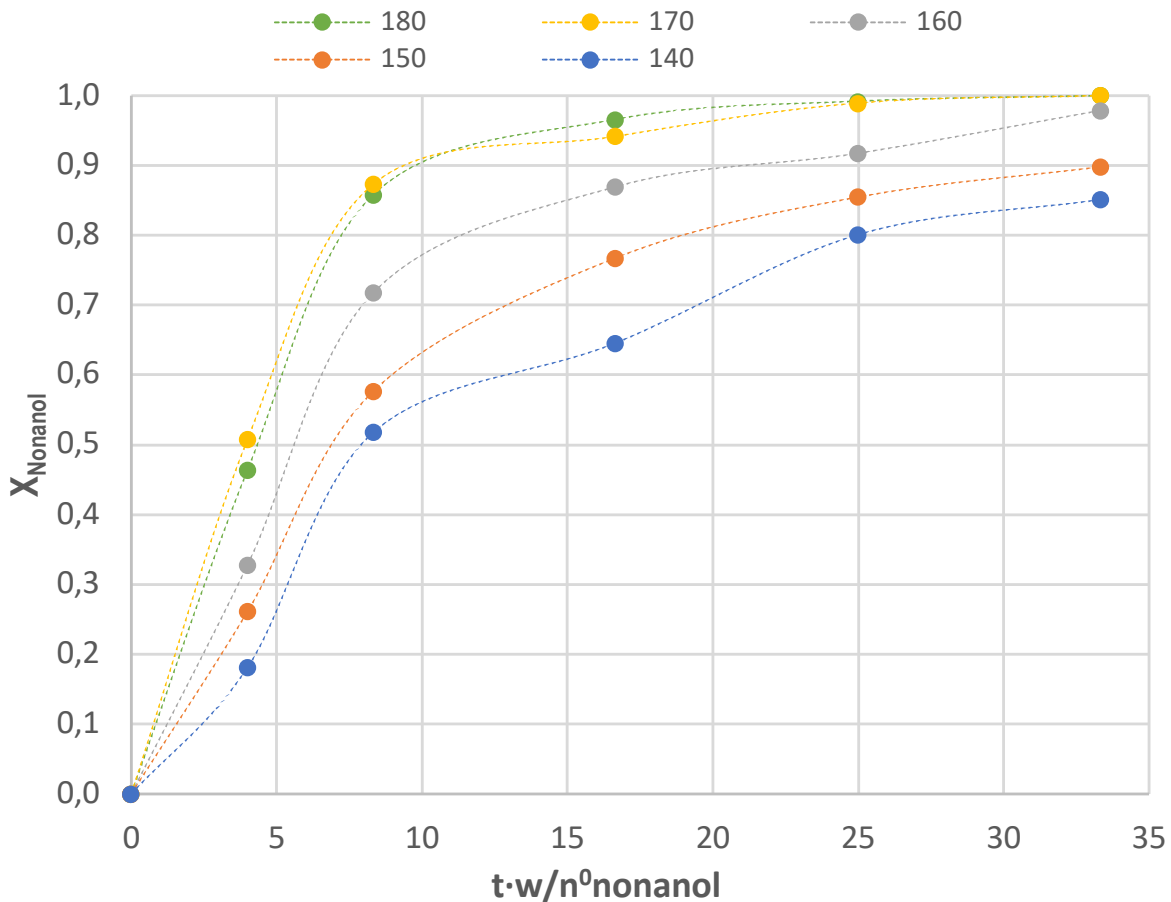


Fig 25. Conversion vs normalized time for different temperatures.

A higher conversion is obtained at a higher operating temperature, as expected since the kinetic constant, according to the Arrhenius equation, increases with temperature and therefore the reaction rate.

In order to clearly observe this relationship, the values of reaction rate versus time have been calculated. Figure 26 shows the effect of temperature over the reaction rate.

The values obtained for an operating temperature of 180°C do not follow the tendency obtained, which was lower than at 170°C. It has been concluded that this is due to an experimental error and therefore, it would be ideal to replicate the experiment in order to prove this result. Due to the current situation of confinement this could not be accomplished.

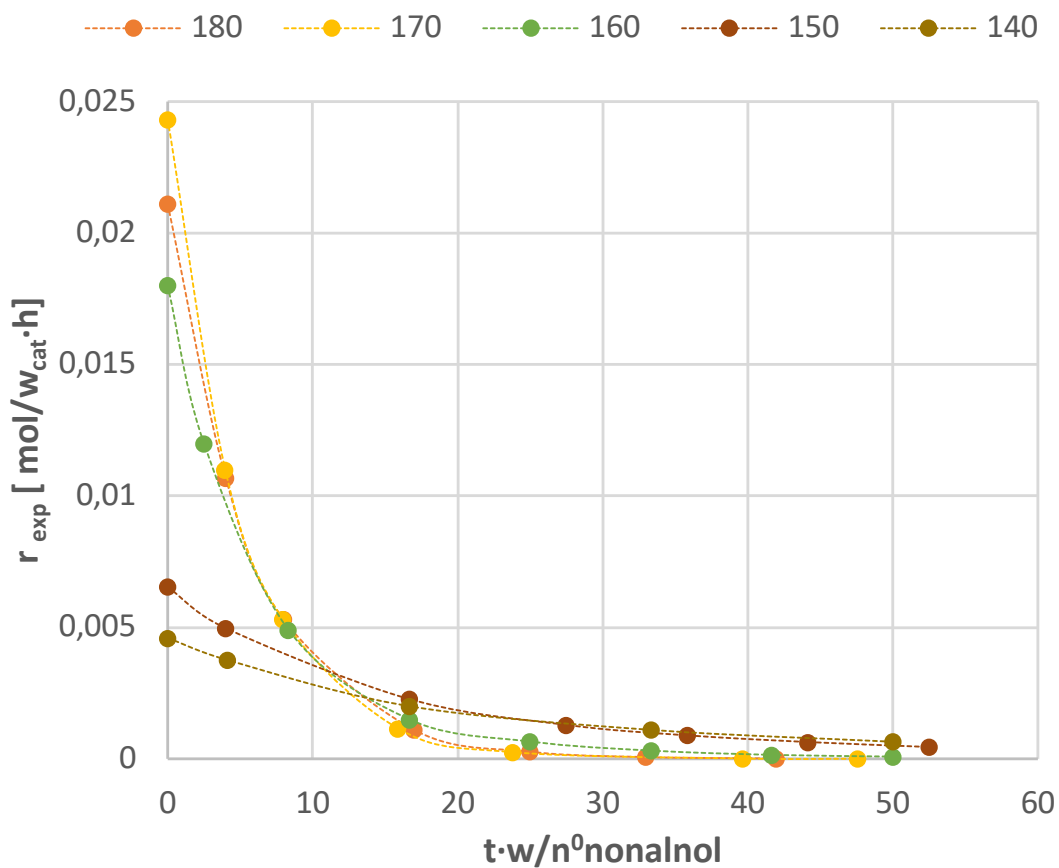


Fig 26. Temperature effect in front the reaction rate.

In order to study the different behaviour between nonenes, the variation of the nonenes relation in terms of the temperature has been analysed in Figure 27.

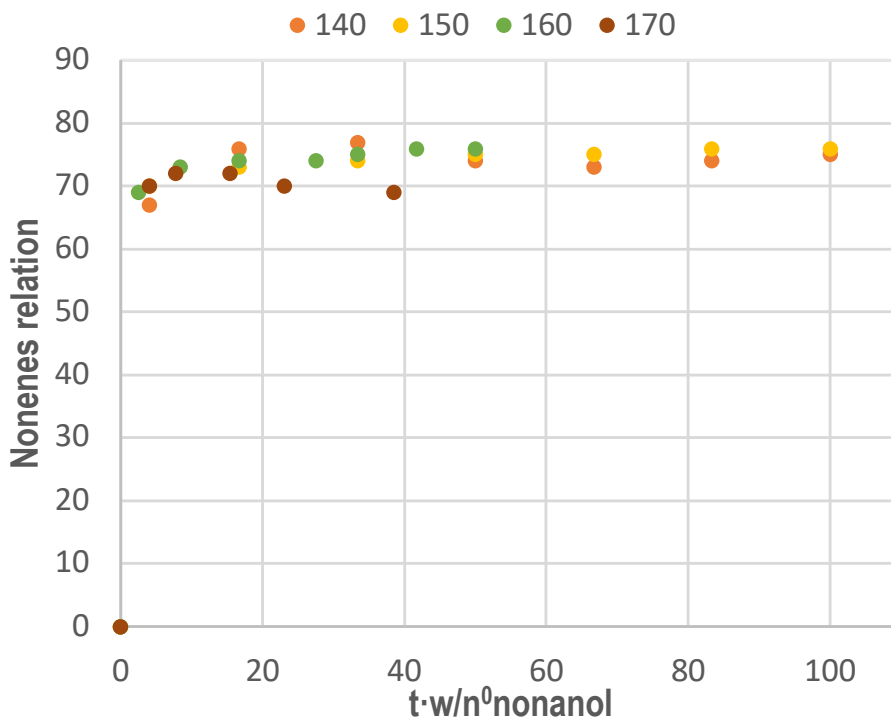


Fig 27. Nonenes relation vs normalized time though different temperatures.

As showed in Figure 27 the relation of nonenes with temperature does not present a clear variation.

## 5.4. DETERMINATION OF APPARENT ACTIVATION ENERGY

Linear regression of Arrhenius equation must be executed by the results of the initial velocity reaction shown in Table 11.

Table 11. Values of temperature (T), 1/T, initial reaction speed ( $r^0$ ) and  $\ln r^0$  used for the determination of  $E_{aapp}$ .

T [K]	$1/T \cdot 10^3$	$r^0$ [mol/ $w_{cat} \cdot h$ ]	$\ln r^0$
413.15	2.420	0.00166	-6.401
423.150	2.363	0.00628	-5.069
433.150	2.309	0.01433	-4.245
443.150	2.257	0.02588	-3.654

Figure 28 shows this regression determining the values of  $E_{aapp}$  and  $A_{app}$ .

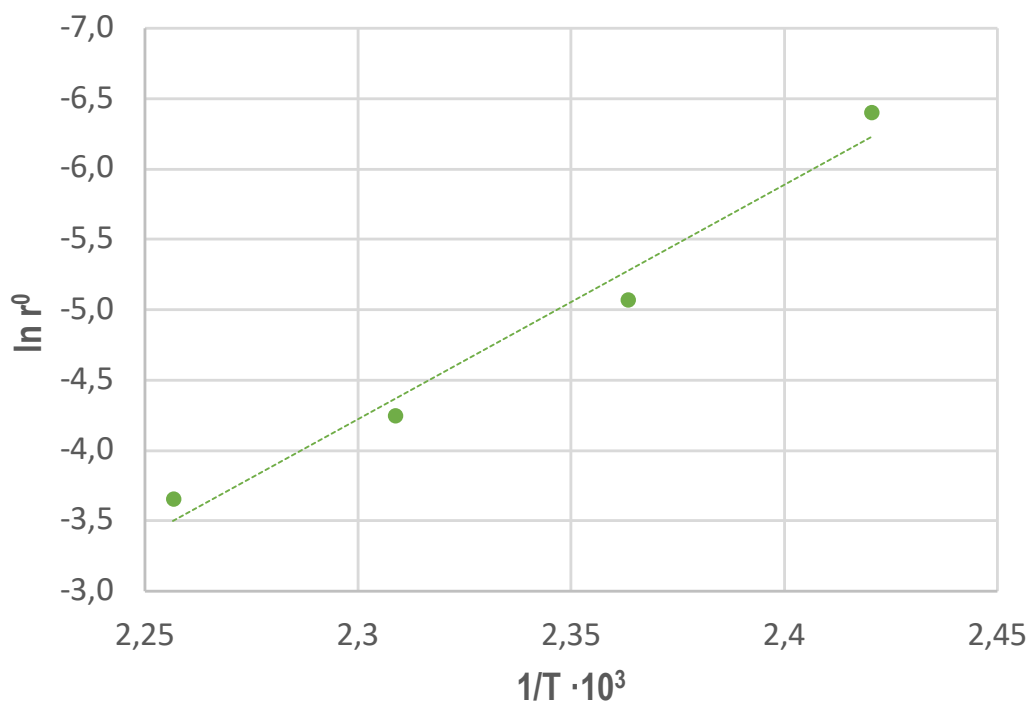


Fig 28. Linear regression for the calculation of  $E_{aapp}$  and  $A_{app}$ .



The values observed in Table 12 are obtained from the linear regression.

Table 12. Values of  $E_{aapp}$  and  $\ln A_{app}$ .

<b><math>E_{aapp}</math> [kJ/mol K]</b>	$138 \pm 8$
<b>LN A</b>	34

The obtained value has been compared with the existing values in the literature for the dehydration of other alcohols. For the dehydration of 1-octanol the apparent energy activation obtained was  $120 \pm 7$  kJ / mol by Casas et al.( 2017). These results are similar to those obtained in our current study, it can be wrap up that the estimated apparent activation energy value is correct.

## 6. CONCLUSIONS

This study has shown that the dehydration reaction of 5-nonanol for the formation of nonenes presents a complete conversion when it is catalyzed by acidic ion exchange resins. This catalyst does not present, the selectivity for the nonenes formation is 100% and therefore it can be considered ideal for obtaining nonenes (all the nonanol consumed goes to the formation of nonenes).

The reaction takes place preferably on the external surface of the catalyst, the different internal properties of the resin do not show an immediate effect on the activity of the catalyst. Therefore, the acid capacity is considered the main propriety. Reaction rate increases significantly as well as the acidic capacity, Amberlyst 35 shows the highest reaction rate.

Furthermore, the effect of temperature on the reaction rate has been studied. The reaction rate increases when working at higher temperatures, as indicated in the Arrhenius equation. Apparent activation energy was estimated with the different reaction speeds calculated at different temperatures with a final result of  $138 \pm 8$  [KJ/mol K].

Overall, it can be concluded that ion exchange resins are extremely efficient for the synthesis of nonenes by the dehydration of 5-nonanol also the fact that are cheaper and more commercially available they are more attractive and for this reason easier to apply at industrial processes.

## REFERENCES AND NOTES:

1. Alonso, D. M., Bond, J. Q., Serrano-Ruiz, J. C., & Dumesic, J. A. (2010). Production of liquid hydrocarbon transportation fuels by oligomerization of biomass-derived C9 alkenes. *Green Chemistry*, 12(6), 992–999. <https://doi.org/10.1039/c001899f>
2. amberlite-amberlyst @ www.sigmaaldrich.com. (n.d.). <https://www.sigmaaldrich.com/chemistry/chemical-synthesis/learning-center/technical-bulletins/al-142/amberlite-amberlyst.html>
3. Ashour, M. K., & Elwardany, A. E. (2020). Addition of two kerosene-based fuels to diesel–biodiesel fuel: Effect on combustion, performance and emissions characteristics of CI engine. *Fuel*, 269(February). <https://doi.org/10.1016/j.fuel.2020.117473>
4. Axelsson, L., Franzén, M., Ostwald, M., Berndes, G., Lakshmi, G., & Ravindranath, N. H. (2008). Perspective: *Jatropha* cultivation in southern India: Assessing farmers' experiences. *Biofuels, Bioproducts and Biorefining*, 6(3), 246–256. <https://doi.org/10.1002/bbb>
5. Balamurugan, T., & Nalini, R. (2016). Experimental investigation on the effect of alkanes blending on performance, combustion and emission characteristics of four-stroke diesel engine. *International Journal of Ambient Energy*, 37(2), 192–200. <https://doi.org/10.1080/01430750.2014.915887>
6. Binod, P., Gnansounou, E., Sindhu, R., & Pandey, A. (2019). Enzymes for second generation biofuels: Recent developments and future perspectives. *Bioresource Technology Reports*, 5(June 2018), 317–325. <https://doi.org/10.1016/j.biteb.2018.06.005>
7. Blanca Torrubia Chalmeta. (2010). Books @ Books.Google.Es. In *Revista Aranzadi de derecho y nuevas tecnologías*. <https://books.google.es/books?id=1rIBBXQhmCwC&printsec=frontcover&dq=termodinamica&hl=es&sa=X&ei=yCsoVeW1F8GLNvySgqAH&ved=0CCEQ6AEwAA#v=onepage&q&f=false>
8. Bringué, R., Fité, C., Iborra, M., Tejero, J., & Cunill, F. (2017). Dehydration of 1-octanol to di-n-octyl ether in liquid phase with simultaneous water removal over ion exchange resins: Effect of working-state morphologies. *Applied Catalysis A: General*, 545(May), 10–16. <https://doi.org/10.1016/j.apcata.2017.07.029>
9. Bringué, R., Ramírez, E., Iborra, M., Tejero, J., & Cunill, F. (2013). Influence of acid ion-exchange resins morphology in a swollen state on the synthesis of ethyl octyl ether from ethanol and 1-octanol. *Journal of Catalysis*, 304, 7–21. <https://doi.org/10.1016/j.jcat.2013.03.006>
10. Casas, C., Bringué, R., Ramírez, E., Iborra, M., & Tejero, J. (2011). Deshidratación de 1-octanol sobre zeolitas y resinas de intercambio iónico. *Ingeniería Química (Spain)*, 43(494), 70–74.
11. Casas, Carlos, Bringué, R., Fité, C., Iborra, M., & Tejero, J. (2017). Kinetics of the Liquid Phase Dehydration of 1-Octanol to Di-n-Octyl Ether on Amberlyst 70. *AIChE Journal*, 63. <https://doi.org/10.1002/aic.15741>
12. Chen, B., Ling, H., & Chang, M. W. (2013). Transporter engineering for improved tolerance

- against alkane biofuels in *Saccharomyces cerevisiae*. *Biotechnology for Biofuels*, 6(1), 1–10. <https://doi.org/10.1186/1754-6834-6-21>
13. Directive, F. Q. (2019). Quality and greenhouse gas intensities of transport fuels in the EU in 2017 (Vol. 2017, Issue 05).
  14. Dong, L., Luo, K., Zhao, L., Zhang, Y., Gao, J., Hao, T., & Xu, C. (2018). Quantitative relationship between olefin saturation and octane loss during HDS process: An insight from molecular structure to experimental activity. *Chemical Engineering Science*, 191, 183–190. <https://doi.org/10.1016/j.ces.2018.06.060>
  15. European Environment Agency. (2019). Greenhouse gas emissions from transport in Europe. European Environmental Agency (EEA), 1. <https://www.eea.europa.eu/data-and-maps/indicators/transport-emissions-of-greenhouse-gases/transport-emissions-of-greenhouse-gases-12>
  16. ExxonMobil Chemical. (n.d.). branched-higher-olefins @ [www.exxonmobilchemical.com](http://www.exxonmobilchemical.com). Retrieved March 2, 2020, from <https://www.exxonmobilchemical.com/en/products/branched-higher-olefins>
  17. Gürbilek, N. (2013). Diesel fuels technical review. *Journal of Chemical Information and Modeling*, 53(9), 1689–1699. <https://doi.org/10.1017/CBO9781107415324.004>
  18. Izquierdo, J. F., Cunill, F., Ejero, J., Iborra, M., & Fité, C. (2004). *Cinética de las reacciones químicas* (EdicionsUniversitat Barcelona) (1st ed., pp. 143–268).
  19. Khaled, A.;Robert, L. (2002). Patent alkenes aromatics.
  20. Li, Y., Liu, H., Song, C., Gu, X., Li, H., Zhu, W., Yin, S., & Han, C. (2013). The dehydration of fructose to 5-hydroxymethylfurfural efficiently catalyzed by acidic ion-exchange resin in ionic liquid. *Bioresource Technology*, 133, 347–353. <https://doi.org/10.1016/j.biortech.2013.01.038>
  21. Maitan-Alfenas, G. P., Visser, E. M., & Guimarães, V. ria M. (2015). Enzymatic hydrolysis of lignocellulosic biomass: Converting food waste in valuable products. *Current Opinion in Food Science*, 1(1), 44–49. <https://doi.org/10.1016/j.cofs.2014.10.001>
  22. Miranda, T., Montero, I., Sepúlveda, F. J., Arranz, J. I., Rojas, C. V., & Nogales, S. (2015). A review of pellets from different sources. *Materials*, 8(4), 1413–1427. <https://doi.org/10.3390/ma8041413>
  23. Parliament, T. H. E. E., & Union, P. (2009). European Parliament Directive 2009/30/EC. *Official Journal of the European Union*, April, L140/88-L140/113.
  24. Pileidis, F. D., & Titirici, M. M. (2016). Levulinic Acid Biorefineries: New Challenges for Efficient Utilization of Biomass. *ChemSusChem*, 9(6), 562–582. <https://doi.org/10.1002/cssc.201501405>
  25. Ramírez, E., Bingué, R., Fité, C., Iborra, M., Tejero, J., & Cunill, F. (2017). Role of ion-exchange resins as catalyst in the reaction-network of transformation of biomass into biofuels. *Journal of Chemical Technology and Biotechnology*, 92(11), 2775–2786. <https://doi.org/10.1002/jctb.5352>
  26. Rosinski, G., & Olsen, C. (2009). Cetane Improvement In Diesel Hydrotreating. *Www.E-Catalysts.Com*, 106, 12–16.
  27. Serrano-Ruiz, J. C., Wang, D., & Dumesic, J. A. (2010). Catalytic upgrading of levulinic acid to 5-nonanone. *Green Chemistry*, 12(4), 574–577. <https://doi.org/10.1039/b923907c>
  28. Shell Chemicals. (n.d.). nonene @ [www.shell.com](http://www.shell.com). Retrieved March 5, 2020, from <https://www.shell.com/business-customers/chemicals/our-products/nonene.html>
  29. Tamás, K., Dénes, K., & Hancsók, J. (2020). Quality improvement of bio-paraffin mixtures. *120(2014)*, 1–7.
  30. Tejero, M. A., Ramírez, E., Fité, C., Tejero, J., & Cunill, F. (2016). Esterification of levulinic acid with butanol over ion exchange resins. *Applied Catalysis A: General*, 517, 56–66. <https://doi.org/10.1016/j.apcata.2016.02.032>

31. Todts, W. (2018). CO<sub>2</sub> emissions from cars: the facts (Issue April). [https://www.dbresearch.de/PROD/DBR\\_INTERNET\\_EN-PROD/PROD000000000346332/CO2+emissions+from+cars:+Regulation+via+EU+Emissio.pdf](https://www.dbresearch.de/PROD/DBR_INTERNET_EN-PROD/PROD000000000346332/CO2+emissions+from+cars:+Regulation+via+EU+Emissio.pdf)
32. Trombettoni, V., Lanari, D., Prinsen, P., Luque, R., Marrocchi, A., & Vaccaro, L. (2018). Recent advances in sulfonated resin catalysts for efficient biodiesel and bio-derived additives production. *Progress in Energy and Combustion Science*, 65, 136–162. <https://doi.org/10.1016/j.pecs.2017.11.001>
33. Werpy, T., & Petersen, G. (2004). *Top Value Added Chemicals from Biomass Volume I. Us Nrel*, Medium: ED; Size: 76 pp. pages. <https://doi.org/10.2172/15008859>
34. Wettstein, S. G., Alonso, D. M., Chong, Y., & Dumesic, J. A. (2012). Production of levulinic acid and gamma-valerolactone (GVL) from cellulose using GVL as a solvent in biphasic systems. *Energy and Environmental Science*, 5(8), 8199–8203. <https://doi.org/10.1039/c2ee22111j>
35. Yan, L., Yao, Q., & Fu, Y. (2017). Conversion of levulinic acid and alkyl levulinates into biofuels and high-value chemicals. *Green Chemistry*, 19(23), 5527–5547. <https://doi.org/10.1039/c7gc02503c>

## ACRONYMS

<b>GVL</b>	$\gamma$ -valero lactone
<b>A45</b>	Amberlyst 45
<b>A35</b>	Amberlyst 35
<b>Dow 2</b>	Dowex 50Wx2.
<b>dp</b>	Particle diameter, mm.
<b>dpore</b>	(macro)pore diameter, mm
<b>DVB</b>	Divinylbenzene
<b>ETBE</b>	Ethyl tert-butyl ether
<b>ISEC</b>	Inverse size exclusion chromatography
<b>LA</b>	Levulinic acid
<b>w</b>	Catalyst mass
<b>R</b>	Molar ratio of 5-nonanol versus dioxane
<b>n</b>	Mol of species
<b>OS</b>	Oversulfonated
<b>MS</b>	Monosulfonate
<b>PS</b>	Polystyrene
<b>t</b>	time
<b>t'</b>	normalized time
<b>T</b>	Temperature, °C, K
<b>Tmax</b>	Maximum work temperature, °C, K
<b>Vsp</b>	Specific volume of swollen polymer, cm <sup>3</sup> /g
<b>X</b>	Conversion of reagent
<b><math>\Sigma</math>Spore</b>	Global (macro)pore surface, m <sup>2</sup> /g
<b><math>\Sigma</math>Vpore</b>	Global (macro)pore volume, cm <sup>3</sup> /g

